INSTITUTE OF FUNDAMENTAL TECHNOLOGICAL RESEARCH
POLISH ACADEMY OF SCIENCES

PHD DISSERTATION

Wave propagation analysis in biological systems

Sławomir Białecki

Doctoral thesis advisor:
Bogdan Kaźmierczak

Warsaw 2024

Acknowledgements

Scientific work is a special kind of activity that can bring extraordinary joy and satisfaction from its various results: understanding what was previously incomprehensible, overcoming uncertainties and difficulties, making discoveries. For this you need an environment and cooperation. I was lucky enough to end up in the outstanding research environment of the Department of Biosystems and Soft Matter of the Institute of Fundamental Technological Research of the Polish Academy of Sciences (IPPT PAN).

Because I've got so much, I would like to express my sincere and deep gratitude to Prof. Bogdan Kaźmierczak - my thesis supervisor, for the proposal of Ph.D. studies subject and research, for the motivating advice and extensive, long-term support during the work on the dissertation, and to Prof. Tomasz Lipniacki - the head of the Department, for the stimulating cooperation, effort and sharing scientific joy.

Many thanks to the management of the Institute for hiring me, for research funding and simulation equipment.

I also sincerely thank my colleagues in the Department of Biosystems and Soft Matter of IPPT PAN for their kindness and constant readiness to help, in particular Dr. Marek Kochańczyk, Pawel Kocieniewski, M.Sc., Prof. Maria Ekiel-Jeżewska, Dr. Beata Hat-Plewińska, Dr.hab. Piotr Korczyk, Dr. Sławomir Błoński, Dr. Joanna Jaruszewicz-Błońska, Dr. Eng. Pawel Nakielski, Krzysztof Zembrzycki, M.Sc.Eng., Dr. Agnieszka Słowicka, Dr.hab. Tomasz Kowalczyk, Dr. Marek Bukowicki, Dr. Marta Gruca, Frederik Grabowski.

I would like to express my special thanks to Paweł Nałęcz-Jawecki, M.Sc., Dominika Hajduk (Nowicka), M.Sc., and Prof. Je-Chiang Tsai for their cooperation and to Prof. Michał Komorowski for giving me access to his computer a few years ago.

An important role in my struggles was played by my family, especially my recently deceased parents and sister. I greatly appreciate the motivating presence from my my ex-spouse, daughters, granddaughters, grandson, brother Paul, his wife Elizabeth and son James, my niece Veronica, and my close neighbour Mrs Anna Danuta Radzikowska.

I think I wouldn't be who I am without being raised by Antonina Jach and her sister - my grandmother Franciszka Jezierska.

Special thanks are due to my friends Krzysztof Śniegula and Piotr Polanowski for their faith in me, which helped me a lot in my decision to apply for doctoral studies.

I am grateful to Professor Maciej Przanowski for the unforgettable scientific cooperation on my master thesis, and to my former boss Prof. Bogdan Nowak (deceased) for helping build my scientific foundation.

Keeping in mind the motto "Either you succeed or you learn", I would like to thank for the educating failures to providence and all those who helped me survive them.

Partial support from the National Science Centre grants: 2014/14/M/NZ6/00537
and 2016/21/B/ST1/03071 is kindly acknowledged.

Streszczenie

Prezentowana rozprawa jest oparta na sześciu pracach [A], [B], [C], [D], [E], [F], które ukazały się w latach 2014-2020.

Celem tych artykułów było zbadanie modeli matematycznych pewnych zjawisk biologicznych, które próbuje się przedstawić jako procesy quasi-oscylacyjne lub propagację fal biegnących. Podstawowymi narzędziami matematycznymi w opisie analizowanych zjawisk są układy równań różniczkowych cząstkowych lub pojedyńcze równania, tzw. równania reakcji-dyfuzji.

Zjawiska oscylacyjne były rozpatrywane na przykładzie czasoprzestrzennej ewolucji stężenia jonów wapniowych zachodzącej wewnątrz komórek eukariotycznych. Zjawiska te związane są z zależną od czasu wymianą jonów wapnia pomiędzy różnymi kompartmentami komórkowymi. Były one rozpatrywane w artykule [A]. Ich analiza opierała się na symulacjach numerycznych w ramach zaproponowanego przez nas rozszerzonego przestrzennie modelu skonstruowanego na bazie modelu cało-kompartmentowego opisywanego układem zwyczajnych równań różniczkowych pierwotnie wprowadzonego w pracy [Marhl, M. *i in.* Complex calcium oscillations and the role of mitochondria and cytosolic proteins. *Biosystems* **57,** 75–86 (2000)]. Model Marhla dotyczy symulacji oscylacji stężenia wapnia uśrednionego po poszczególnych kompartmentach komórki eukariotycznej.

W modelu przestrzennym ewolucja stężenia wapnia w punkcie zależy od jego położenia w kompartmencie. Jednak dla dużych wartosći współczynnika dyfuzji przebiegi czasowe stężenia wapnia w różnych punktach kompartmentu przestają się od siebie różnić i stają się podobne do odpowiadającym im przebiegów w modelu cało-kompartmentowym. Z kolei, dla malejących wartości współczynników dyfuzji przebiegi te stają się coraz bardziej chaotyczne, zanim zupełnie znikną dla odpowiednio małego współczynnika dyfuzji.

Równania różniczkowe cząstkowe opisujące wspomniane wyżej buforowane układy wapniowe są przykładami równań reakcji-dyfuzji, które są jednym z głównych narzędzi biologii matematycznej. Jedną z podstawowych klas rozwiązań takich układów są fale biegnące [Volpert, A. I., Volpert, V. A. & Volpert, V. A. *Traveling Wave Solutions of Parabolic Systems* (American Mathematical Society, 1994)]. Są one ważne z tego względu, że mogą opisywać procesy propagacji sygnałów biologicznych. Najczęściej zjawiska takie są w przybliżeniu modelowane przez quasi-jednowymiarowy opis odpowiadający falom płaskim. To założenie redukuje wiele trudności technicznych związanych z matematyczną analizą tych procesów. Często jednak przybliżenie takie jest zbyt upraszczające. Jest tak w przypadku procesów zachodzących na powierzchniach zakrzywionych np. na błonie komórkowej analizowanych w publikacjach [B], [C], [E]. W pracach tych rozpatrzona została transdukcja sygnałów biologicznych jako propagacja fali biegnącej po powierzchni membrany komórkowej. Fala taka może powodować aktywację komórek (albo ich dezaktywację). Przykładami takich zjawisk są w szczególności procesy aktywacji komórek układu odpornościowego (limfocytów typu B) zachodzące na ich błonach, omawiane w przytoczonych pracach oraz zawartych w nich referencjach. Stosując uproszczony model opisywany przez skalarne równanie reakcji dyfuzji z przedziałami liniowym członem źródłowym w postaci McKeana potrafimy scharakteryzować procesy aktywacji na membranie komórkowej opisywanej (po odpowiednim skalowaniu) przez dwuwymiarową sferę jednostkową.

W pracy [B] zostało znalezione niestabilne stacjonarne rozwiązanie powyższego równania mające własność separatrysy pomiędzy dwoma zbiorami warunków początkowych, które propagują się odpowiednio do jednorodnego stanu aktywnego albo do jednorodnego stanu nieaktywnego na błonie komórkowej. Uzyskany rezultat jest, naszym zdaniem, bardzo interesujący z matematycznego punktu widzenia, ponieważ separatrysa została znaleziona w postaci analitycznej. Ma także znaczenie poznawcze, gdyż pozwala stwierdzić istnienie minimalnego obszaru stymulacji początkowej zapewniającego aktywację całej komórki.

W pracy [C] analizowane jest równanie zależne od czasu, którego stacjonarny odpowiednik został przeanalizowany w [B]. Zawiera ona techniczne przygotowanie do analizy istnienia i własności rozwiązań typu "mild solutions" będących przedmiotem trzeciego artykułu [E]. W pracy [C], przy założeniu istnienia słabych rozwiązań, pokazujemy między innymi, że rozwiązanie należące do klasy $C^0([0,T],L^2((0,\pi)))$ należy jednocześnie do klasy $C^{1,\beta}_{x,t}([0,\pi]\times[0,T])$, dla $\beta\in(0,1/4)$ tzn. jest C^1 gładkie ze względu na współrzędną przestrzenną i ciągłe Hölderowsko ze względu na zmienną czasową

z wykładnikiem β w przedziale $(0, 1/4)$.

W artykule [E] kontynuujemy badanie zjawiska propagacji fal na kuli dla wspomnianego wyżej modelu aktywacji komórek biologicznych. Na wstępie pokazujemy istnienie i jednoznaczność rozwiązań typu mild solutions dla liniowego parabolicznego problemu początkowo - brzegowego z odpowiednio zadaną funkcją źródłową $f(x,t)$, zakładając, że rozwiązania te są dane przez rozwinięcie w szereg wielomianów Legendre'a. Aby scharakteryzować gładkość rozwiązań, znajdujemy jednostajne oszacowania na współczynniki tego rozwinięcia względem zmiennej przestrzennej x. Istotną trudnością w tej analizie jest nieciągłość względem zmiennej przestrzennej x wyrazu źródłowego implikowana przez własności funkcji McKeana w pierwotnej wersji równania i uniemożliwiającą wykorzystanie standardowych twierdzeń do uzyskania dowodu istnienia, jedyności i gładkości rozwiązań. Dowód ten w ogólności w przypadku nieliniowym otrzymujemy następnie stosując zmodyfikowaną metodę kolejnych przybliżeń oraz twierdzenie o istnieniu rozwiązań dla przypadku liniowego. Skonstruowane rozwiązania są klasy $C^{2,1}$ wszędzie poza punktem odpowiadającym nieciągłości wyrazu źródłowego. Następnie konstruujemy parę zależnych od czasu super- i sub-rozwiązań, które imitują monotoniczne profile frontów fal biegnących wzdłuż południków z pewną prędkością. W oparciu o skonstruowaną wcześniej metodę dowodu dowodzimy istnienia rozwiązania, które ma charakter fali biegnącej poruszającej się z prędkością zależną od czasu i położenia na kuli.

Ten rodzaj analizy pozwala stwierdzić, że warunki początkowe są dobrze określone i jeśli są większe niż wartość stanu progowego, rozwiązanie propaguje się w czasie w kierunku jednorodnego stanu ustalonego o większej wartości. Jeśli natomiast warunki początkowe są mniejsze niż warunek progowy, to rozwiązanie zbiega się do zerowego stanu ustalonego. Wartości stanu progowego są zadane przez niestabilne rozwiązanie stacjonarne znalezione w pracy [B].

Publikacje [D] i [F] poświęcone są analizie wpływu geometrii trójwymiarowych obszarów na propagację fal biegnących wewnątrz ich objętości ([D]) badź też po ich powierzchni ([F]).

W pracy [D] proponujemy między innymi model polaryzacji trójwymiarowych kanałów na skutek zatrzymywania się frontów fal biegnących (wewnątrz kanałów) w sąsiedztwie wklęsłych fragmentów powierzchni ich brzegu, w miejscu ich rozszerzającego się przekroju.

Powstanie zjawiska stacjonarnego i stabilnego czoła fali biegnącej chcemy właśnie interpretować jako modelowy mechanizm łączący kształt brzegu obszaru z polaryzacją jego wnętrza. Jak wykazaliśmy numerycznie, można w ten sposób wygenerować złożone konfiguracje polaryzacyjne na zbiorach opisujących różnorodne obiekty biologiczne. Zaproponowany model wyróżnia się istotnie na tle innych mechanizmów tworzenia się wzorców przestrzennych (pattern formation). W przeciwieństwie do nich, np. mechanizmu opartego na bifurkacji Turinga, opisany jest bowiem pojedynczym równaniem typu reakcji-dyfuzji. Co więcej, powiązanie polaryzacji z geometrią obszaru, czyni go doskonałym narzędziem opisu zjawisk polaryzacyjno-segmentacyjnych w trakcie procesów morfogenezy organizmów biologicznych.

W pracy [F] udowadniamy, że podobne zjawiska mogą charakteryzować propagację fal biegnących na hiperpowierzchniach dwuwymiarowych. Pokazujemy w niej, że heteroklinicznyfront fali biegnącej, rozchodzący się po dwuwymiarowym brzegu trójwymiarowego obszaru może zatrzymywać się na jego wklęsłych kawałkach wzdłuż linii odpowiadających stałej krzywiźnie geodezyjnej. Zjawisko to możemy uważać za jeden z możliwych mechanizmów polaryzacji hiperpowierzchni w procesach dających się opisać równaniami typu reakcji dyfuzji. Co więcej, polaryzacja brzegu może implikować polaryzację całego obszaru trójwymiarowego. Praca uzupełniona jest teoretyczną analizą warunków stabilności tego rodzaju rozwiązań w zależności od lokalnych własności geometrycznych rozpatrywanej hiperpowierzchni.

Teoretyczne rezultaty zawarte w obu pracach mają charakter asymptotyczny, gdyż zakładają one zaniedbywalną grubość frontu falowego (tzn. szerokość, na której wartość opisywanej wielkości zmienia się efektywnie między swoimi wartościami stacjonarnymi), tak aby (asymptotycznie) mógł on być utożsamiony z hiperpowierzchnią (w przypadku 3D) lub linią (w przypadku fal na powierzchni 2D). Nakłada to pewne warunki na występujące w rozpatrywanym równaniu parametry i funkcje. W szczególności odnosi się to do małości współczynnika dyfuzji oraz do postaci funkcji źródłowej. Przedstawione w pracy symulacje numeryczne dowodzą jednak, że opisane efekty polaryzacyjne mają miejsce w stosunkowo szerokim zakresie vartości parametrów i mogą być spełnione w przypadku wielu zjawisk biologicznych.

Abstract

The presented dissertation is based on six papers [A], [B], [C], [D], [E], [F], which were published between 2014 and 2020.

The aim of these articles was to investigate mathematical representation of certain biological phenomena as quasi-oscillatory processes or traveling wave propagation. The basic mathematical tools in the description of the analyzed phenomena are systems of partial differential equations or single one, the so-called reaction-diffusion equations.

Oscillatory phenomena were analysed by considering the example of spatio-temporal evolution of calcium ion concentration occurring inside eukaryotic cells. These phenomena are related to the time-dependent exchange of calcium ions between different cellular compartments. They were considered in the article [A]. Their analysis was based on numerical simulations within the spatially extended model proposed by us, constructed on the basis of the whole-compartment model described by the system of ordinary differential equations originally introduced in [Marhl, M. *et al.* Complex calcium oscillations and the role of mitochondria and cytosolic proteins. *Biosystems* **57,** 75–86 (2000)]. The Marhl's model deals with the simulation of calcium concentration oscillations averaged over individual compartments of an eukaryotic cell.

In the spatial model, the evolution of the calcium concentration at a point depends on its position in the compartment. However, for large values of the diffusion coefficients, the time courses of calcium concentration in different points of the compartment cease to differ from each other and become similar to the corresponding courses in the whole-compartment model. In turn, for decreasing values of diffusion coefficients, the waveforms of oscillations become more and more chaotic, and finally they disappear completely for a sufficiently small diffusion coefficient.

The partial differential equations describing the above-mentioned buffered calcium systems are examples of reaction-diffusion equations, which are one of the main tools of mathematical biology.

Traveling waves [Volpert, A. I., Volpert, V. A. & Volpert, V. A. *Traveling Wave Solutions of Parabolic Systems* (American Mathematical Society, 1994)] are one of the basic classes of solutions for such systems. They are important because they can describe the propagation processes of biological signals. Most often, such phenomena are approximately modeled by a quasi-one-dimensional description corresponding to plane waves. This assumption reduces many of the technical difficulties associated with the mathematical analysis of these processes. However, this approximation is often too simplistic, as in the case of processes occurring on curved surfaces, e.g. on the cell membrane, as were analysed in the papers [B], [C], [E]. In these papers, the transduction of biological signals was considered as the propagation of a traveling wave along the surface of the cell membrane. Such a wave can cause cell activation or deactivation. Examples of such phenomena are, in particular, the processes of activation of immune cells (type B lymphocytes) taking place on their membranes, considered in the mentioned above papers and the references therein. Using a simplified model described by a scalar reaction-diffusion equation with a piecewise linear source term in the McKean form, we were able to characterize the activation processes on the cell membrane described (after appropriate scaling) by a two-dimensional unit sphere.

In the work [B], an unstable stationary solution of the above equation was found having the property of separatrix between the two sets of initial conditions that propagate either to a homogeneous active or inactive state on the cell membrane. The obtained result is, in my opinion, very interesting from a mathematical point of view, because the separatrix was found in an analytic form. It is also interesting from a practical point of view, because it allows to determine the existence of a minimum area of initial stimulation ensuring the activation of the whole cell.

In the paper [C] we analyze a time-dependent equation whose stationary counterpart was analyzed in the paper [B]. It contains a technical preparation for the analysis of the existence and properties of the "mild solutions" to this equation, which is the subject of the third article [E]. In the work [C], assuming the existence of weak solutions, we show, among other things, that a solution belonging to the class $C^0([0,T], L^2((0,\pi)))$ also belongs to the class $C^{1,\beta}_{x,t}([0,\pi]\times[0,T])$, for $\beta \in (0,1/4)$, i.e. is C^1 smooth in terms of the space coordinate and Hölder continuous in terms of the time variable with the exponent β in the interval $(0,1/4)$.

In the article [E], we continue the study of the phenomenon of wave propagation on a sphere for the aforementioned biological cell activation model. First, we show the existence and unambiguity of "mild solutions" for the linear parabolic initial - boundary value problem with an appropriately given source function $f(x,t)$, assuming that the solutions are given by expansion into a series of Legendre polynomials. To characterize the smoothness of the solutions, we find uniform estimates for the coefficients of this expansion with respect to the spatial variable x. A significant difficulty in this analysis is the x-discontinuity of the source expression implied by the properties of the McKean function in the original version of the equation and making it impossible to use standard theorems to deduce the existence, uniqueness, and regularity of solutions. This proof in general in the nonlinear case is then obtained using the modified method of successive approximations and the existence of solutions for the linear case. The constructed solutions are of class $C^{2,1}$ everywhere except the point corresponding to the discontinuity of the source term. We then construct a pair of time-dependent super- and sub-solutions that imitate the monotonic profiles of a traveling wave fronts moving along the meridians at a certain speeds. Based on the method of proof constructed there, we demonstrate the existence of a solution, having the character of a traveling wave moving at a speed depending on time and position on the sphere.

This type of analysis allows us to conclude that the initial conditions are well defined and if bigger than the threshold state value, the solution propagates towards a higher homogeneous steady state over time. If, on the other hand, the initial conditions are smaller than the threshold condition, then the solution converges to the zero steady state. The threshold state is given by an unstable stationary solution.

The publications [D] and [F] are devoted to the influence of the surface curvature of the boundary of a 3D region on a wave traveling inside the volume the region or on its surface.

In the work [D], we propose, among other things, a model for the polarization of the 3D channels due to the stopping/pinning of wave fronts running inside the channel near the widening concave parts of its boundary. We want to interpret the emergence of the phenomenon of a stationary and stable traveling wave front as a model mechanism connecting the shape of the boundary of the region with the polarization of its interior. As we have demonstrated numerically, complex polarization configurations can be generated in this way on domains describing a variety of biological objects. The proposed model stands out significantly from other spatial pattern formation mechanisms. In contrast to them, e.g. the mechanism based on Turing bifurcation, it is described by a single equation of reaction-diffusion type. Moreover, the link between polarization and region geometry makes it an excellent tool for describing polarization-segmentation phenomena during morphogenesis processes in biological organisms. The place where wave front line is pinned, is specified analytically and numerically demonstrated in axially symmetric case.

In the paper [F] we prove that very similar phenomena can characterize the propagation of traveling waves on two-dimensional hypersurfaces. In it, we show that a heteroclinic traveling wave front propagating along a 2D boundary surface of a 3D region of a channel can stop on its concave pieces nearby lines corresponding to a constant geodesic curvature. We can consider this phenomenon as one of the possible mechanisms of hypersurface polarization in processes that can be described by equations of reaction-diffusion type. Moreover, 2D boundary polarization can imply polarization of the whole 3D region. The work is complemented by a theoretical analysis of the stability conditions for such solutions depending on the local geometrical properties of the considered hypersurface.

The theoretical results contained in the papers [D] and [F] assume negligible thickness of the wave front (i.e. a width over which the value of the described magnitude changes effectively between its stationary values), so that (asymptotically) it can be identified with a hypersurface (in the 3D case) or a line (in the case of waves on 2D surfaces). This imposes certain conditions on the parameters and functions in the equation under consideration. In particular, this relates to the smallness of the diffusion coefficient and the form of the source function. However, the numerical simulations presented in this paper prove that the described polarization effects take place over a relatively wide range of parameter values and can be fulfilled in the case of many biological phenomena.

Contents

Analiza zjawisk propagacji fal w systemach biologicznych

Wstęp

Od kilku dziesięcioleci biologia przejmuje rolę głównego nurtu badań naukowych, stając się przy okazji inspiracją i motywacją badań w wielu innych dziedzinach, a w szczególności w zakresie modelowania matematycznego. Badanie i analiza układów biologicznych jest utrudniona przez ich gigantyczną złożoność i, ogólnie rzecz biorąc, nieliniowy charakter zachodzących w nich procesów. Jedną z najbardziej obiecujących strategii poznawczych układów biologicznych jest konstrukcja modeli matematycznych poprzez porównanie z eksperymentem rezultatów symulacji komputerowych opartych na tych modelach. Niestety, w chwili obecnej symulacje numeryczne realizowane np. w ramach dynamiki molekularnej czy też zaawansowanych procesów stochastycznych, potrafią wyjasnić tylko pojedyncze aspekty zjawisk biologicznych zachodzacych wewnątrz nawet najprostszych komórek eukariotycznych. Wynika to z faktu ogromnej wielopoziomowej złożoności geometrycznej i fizyko-chemicznej komórek oraz innych struktur biologicznych, implikującej bardzo długie czasy symulacji komputerowych w zakresie modeli matematycznych uwzględniających podstawowe procesy wewnątrz komórkowe. W konsekwencji, zachodzi potrzeba wypracowania metodyki analizy zjawisk biologicznych w oparciu o modele uproszczone. Jednym z takich uproszczeń jest opis zjawisk biologicznych w języku równań różniczkowych cząstkowych. Wśród nich wyróżnić należy układy równań cząstkowych typu reakcji dyfuzji, które w swej podstawowej wersji można uważać za podklasę układów równań parabolicznych, bądź też eliptycznych w przypadku stacjonarnym. Z matematycznego punktu widzenia układy te są stosunkowo dobrze poznane [3], [2], [4], [5], [6], przy czym warto dodać, że wiele uogólnień, nowych problemów i metod związanych z tymi równaniami zostało zainspirowanych właśnie zjawiskami biologicznymi. Z drugiej strony, ich struktura pozwalająca uwzględnić podstawowe procesy biologiczno-fizyczno-chemiczne zachodzące w komórkach, tkankach, pojedynczych organizmach żywych, a nawet całych ekosystemach, nadaje się doskonale do opisu i czasoprzestrzennej analizy całego spektrum procesów biologicznych, takich jak embrio- i morfogeneza, przesyłanie informacji biologicznej, rywalizacja miedzygatunkowa, itp. Jednym z przykładów zastosowań układów równań typu reakcji-dyfuzji jest modelowanie procesów chondrogenicznych, tzn. procesów tworzenia sie struktur kostnych w trakcie rozwoju morfogenetycznego kręgowców [7]. Inne przykłady dotyczą zagadnień poruszania się mikroorganizmów wskutek zmieniającego się w czasie stężenia odpowiedniego morfogenu [8], [9], [10], formowania się struktur przestrzennych populacji bakterii lub ameb na skutek chemotaksji [11], [12], [13], [14], czy też opisu rozprzestrzeniania się infekcji. Ciągle aktualnymi i uzupełniającymi się źródłami zagadnień biologii matematycznej pozostają książki: [3] i [15]. W pracach będących przedmiotem powyższej dysertacji do modelowania i analizy wybranych zjawisk biologicznych stosujemy właśnie aparat matematyczny rozwinięty dla układów równań typu reakcji-dyfuzji. Prace te poświęcone są w ogólności procesom transdukcji sygnałów biologicznych odbywających się wewnątrz obszarów o skomplikowanej strukturze przestrzennej oraz na ich powierzchniach ograniczających, które możemy utożsamiać z membranami komórkowymi, lub brzegami innych tworów biologicznych. Powyższe procesy opisywane są lokalnie przez rozwiązania równań reakcji-dyfuzji o charakterze fal biegnących, które w przeciwieństwie do fal rozchodzących się w prostoliniowych cylindrach o stałym przekroju mogą objawiać się dodatkowymi zjawiskami, istotnymi również z biologicznego punktu widzenia.

Cele i ogólna charakterystyka rezultatów pracy

Celem przedstawionej rozprawy doktorskiej jest matematyczna i numeryczna analiza procesów oscylacyjnych oraz procesów propagacji sygnałów w układach biologicznych. Procesy takie stanowią dwa podstawowe scenariusze w ramach deterministycznego opisu zjawisk ewolucyjnych. Przykładem procesów oscylacyjnych są powtarzające się w czasie przestrzenne zmiany stężenia substancji biochemicznych zachodzące wewnątrz komórek biologicznych. Jednym z najważniejszych wewnątrzkomórkowych czynników biologicznych jest wapń. Odpowiednie stężenie jonów wapniowych w cytozolu komórkowym jest niezbędnym warunkiem prawidłowego funkcjonowania komórki. Problemem, jaki postawiliśmy sobie w tym przypadku była odpowiedź na pytanie: Czy dla typowych komórek biologicznych oscylacje stężenia jonów wapniowych mogą być opisywane tzw. modelami kompartmentowymi? Zagadnienie to zbadaliśmy, poprzez uogólnienie znanego modelu kompartmentowego bazującego na równaniach różniczkowych zwyczajnych na przypadek przestrzenny 3D, opisany przez równania różniczkowe cząstkowe. W szczególności zbadaliśmy wpływ współczynnika dyfuzji wapnia na charakter rozwiązań. W przypadku symulacji 3D zaobserwowaliśmy m.in. niezwykle złożone zachowanie się rozwiązań oscylacyjnych w miarę malenia współczynnika dyfuzji jonów wapnia, oraz ich zanikanie przy jego dostatecznie małej wartości. Jak wiadomo, wapń jest jednym z najważniejszych czynników sygnałowych. Przekazywanie informacji realizuje się przede wszystkim poprzez różnego rodzaju fale stężenia wapnia. Matematyczna teoria fal biegnących w modelach opisywanych za pomocą nieliniowych równań typu reakcji-dyfuzji jest już bardzo dobrze opracowana dla obszarów *de facto* jednowymiarowych (idealnych cylindrów o stałym przekroju). Podejście takie jest bardzo dobrze uzasadnione w przypadku fal poruszających się w długich komórkach biologicznych, takich jak komórki mięśniowe, staje się jednak nieadekwatne w przypadku fal poruszających się po zakrzywionych powierzchniach, takich jak membrany komórkowe. (Krzywizna wpływa tutaj istotnie na własności funkcji opisującej transdukcję sygnału.) Mogą to być np. fale wapniowe propagujące się na powierzchni zapłodnionego oocytu, lub też fale aktywacji receptorów i odpowiadających im kinaz np. na powierzchni limfocytów typu B. Zaaktywowane kinazy wpływają na stan komórki przesyłając informację do jądra. Odpowiednio silny sygnał przełącza komórkę ze stanu nieaktywnego do aktywnego, umożliwiając jej reakcję na bodźce zewnętrzne. Zadaniem, które postawiliśmy przed sobą w tym zakresie, była matematyczna analiza równania typu reakcji-dyfuzji opisującego powyższy proces na sferze modelujacej membranę komórkową z uproszczoną kawałkami liniową funkcją źródłową. Praca nad realizacją postawionego zadania zaowocowała znalezieniem rodziny ścisłych rozwiązań stacjonarnych rozpatrywanego równania wyrażonych poprzez funkcje hipergeometryczne Gaussa. Funkcje te stanowią separatrysy określające minimalną wielkość klastra zaaktywowanych receptorów, która zapewnia całkowitą aktywację komórki. Pozwalają również na badanie efektów progowych w zależności od parametrów modelu. W oparciu o powyższe funkcje mogliśmy następnie zdefiniować sub- i super-rozwiązania rozpatrywanego równania, a następnie udowodnić istnienie rozwiązania mającego cechy fali biegnącej aktywującej membranę komórkową.

Nieskończony cylinder prostoliniowy o stałym przekroju jest specyficznym zbiorem geometrycznym o wysokiej symetrii. Można się zatem spodziewać, że propagacja fal odbywająca się w bardziej ogólnych zbiorach trójwymiarowych, lub na ich powierzchniach granicznych, będzie charakteryzować się szeregiem własności, które nie mają swoich odpowiedników dla idealnych cylindrów. Niektóre z tych własności zostały pokazane w dwóch koautorskich pracach dotyczących właśnie propagacji fal na wklęsłych zbiorach 3D oraz na powierzchniach zakrzywionych 2D. W pracach tych wykazaliśmy numerycznie, że w obu przypadkach propagujące się fale mogą zatrzymywać się na wklęsłych częściach swoich nośników. W ten sposób może dokonywać się stabilna polaryzacja dwu- i trójwymiarowych obszarów, w szczególności wielu struktur biologicznych. Taki mechanizm polaryzacyjny może mieć duże znaczenie w modelach morfogenetycznych. Polaryzacja struktury jest tutaj bowiem zależna od jej geometrii, a modyfikacje geometryczne od aktualnej polaryzacji. Co więcej, w przeciwieństwie do innych mechanizmów dyferencjacji przestrzennych, powyższy mechanizm polaryzacyjny generowany jest przez pojedyncze równanie typu reakcji-dyfuzji.

Wave propagation analysis in biological systems

Introduction

For several decades, biology has taken over the role of mainstream scientific research, additionally becoming the inspiration and motivation for research in many other fields, especially in the field of mathematical modeling. Unfortunately, the study and analysis of biological systems is restrained by their gigantic complexity and, in general, the nonlinear nature of the processes considered. One of the most promising cognitive for biological systems is to construct mathematical models by comparing experiments with the results of computer simulations based on these models. However, at present, numerical simulations realized, for example, in the framework of molecular dynamics or advanced stochastic processes, are able to explain only single aspects of biological phenomena occurring inside even the simplest eukaryotic cells. This is due to the fact of the enormous multilevel geometric and physico-chemical complexity of cells and other biological structures, implying very long times for computer simulations of mathematical models that take into account the basic processes inside the cell. Consequently, there is a need to develop a methodology for analyzing biological phenomena based on models, which are simplified. One such simplification is the description of biological phenomena in the language of partial differential equations. Among these are systems of partial differential equations of the reaction-diffusion type, which in their basic version can be considered a subclass of systems of parabolic equations (or elliptic in the stationary case). From a mathematical point of view, these systems are relatively well understood (see [3], [2], [4], [5], [6]), with the noteworthy fact that many of the generalizations, new problems and methods associated with these equations were inspired precisely by biological phenomena. On the other hand, their structure, enabling to take into account the basic biological-physical-chemical processes in cells, tissues, individual living organisms and even entire ecosystems, is perfectly suited for the description and spatio-temporal analysis of the entire spectrum of biological processes, such as embryo- and morphogenesis, transmission of biological information, interspecies competition, etc. One example of applications of systems of reaction-diffusion type equations is the modeling of chondrogenic processes, i.e., the processes of bone structures formation during the morphogenetic development of vertebrates [7]. Other examples address issues of how microorganisms move as a result of time-varying concentration of the corresponding morphogen [8], [9], [10], the formation of spatial structures of populations of bacteria or amoebae due to chemotaxis [11], [12], [13], [14], or the description of the spread of infection. Continuously up-to-date and complementary sources of problems in mathematical biology remain the books: [3] and [15].

In the papers constituting the dissertation, we use the mathematical apparatus developed for systems of reaction-diffusion equations to model and analyze selected biological phenomena. These works are devoted, in general, to the processes of transduction of biological signals inside complex spatial structure and on their bounding surfaces, which we can identify with cell membranes, or the boundaries of other biological entities. The above-mentioned processes are described locally by solutions of reaction-diffusion equations in the form of traveling waves, which, unlike waves propagating in rectilinear cylinders with constant cross-sections, can manifest additional phenomena, also important from the biological point of view.

Objectives and general characteristics of the results

The aim of the presented dissertation is the mathematical and numerical analysis of oscillatory processes and signal propagation processes in biological systems. Such processes represent two basic scenarios within the deterministic description of evolutionary phenomena. An example of oscillatory processes are (repeating over time) spatial changes in concentrations of biochemical substances occurring inside biological cells. One of the most important intracellular biological factors is calcium. An adequate concentration of calcium ions in the cell cytosol is a prerequisite for the proper functioning of the cell. The task we undertook in this case was to answer the question: Can, for typical biological cells, oscillations of calcium ion concentration be described by so-called compartmental models? We investigated this problem by generalizing an existing compartmental model based on ordinary differential equations to the spatially 3D model described by partial differential equations. In particular, we investigated the influence of the calcium diffusion coefficient on the nature of its solutions. In the case of 3D simulations we observed, among others, the extremely complex behavior of oscillatory solutions as the diffusion coefficient of calcium ions decreases, and disappearance of oscillations as diffusion achieves sufficiently small value. As is well known, calcium is one of the most important signaling factors. Transmission of information is realized primarily via various types of waves of calcium concentration. The mathematical theory of traveling waves in the models described by means of nonlinear reaction-diffusion equations is very well developed, however only for *de facto* one-dimensional domains (ideal cylinders of constant cross-section). This kind of approximation is very well justified for waves moving in long biological cells, such as muscle cells, but becomes inadequate for waves traveling on curved surfaces, such as membranes of cells. (The curvature, in this case, significantly affects the signal transduction.) Examples of such waves can include, e.g. calcium waves propagating on the surface of a fertilized oocyte, or activation waves of receptors and their corresponding kinases on the surface of B-type lymphocytes. The activated kinases affect the state of the cell by sending information to the nucleus. A sufficiently strong signal switches the cell from an inactive state to an active one, enabling it to respond to external stimuli. The task we undertook in this case was the mathematical analysis of the reaction-diffusion equation describing the above process on the sphere modeling the cell membrane with a simplified piece-wise linear source function. The work on the implementation of this plan resulted in finding a family of strict stationary solutions to the considered equation expressed explicitly by the Gaussian hypergeometric functions. The constructed functions have the separatrix property and determine the minimum size of the cluster of activated receptors, which ensures the complete activation of the cell. They also enable us to establish activation thresholds with respect to the parameters of the model. Based on the above functions, we were then able to define sub- and super-solutions of the considered equation, and then prove the existence of a solution having the characteristics of a traveling wave activating the cell membrane. An infinite rectilinear cylinder of constant cross-section is a specific geometric set with very high symmetry. It can therefore be expected that wave propagation taking place in more general three-dimensional sets, or on their boundary surfaces, will be characterized by a number of properties that do not have their counterparts for ideal cylinders. Some of these properties have been shown in two coauthored papers dealing exactly with waves' propagation inside concave 3D sets and on 2D curved surfaces. In these works, we showed numerically that in both cases, propagating waves can stop at concave parts of their carriers. In this way, stable polarization of 2- and 3-dimensional regions, in particular of many biological structures, can arise. Such a polarization mechanism can have crucial applications in morphogenetic models. The polarization of the structure depends here on its geometry, and the geometric modifications on the polarization. Moreover, unlike other spatial differentiation mechanisms, the above polarization mechanism is generated by a single reaction-diffusion equation.

Articles constituting the thesis

This thesis consists of the following six original articles:

A **Calcium Oscillations in a Spatially Extended Three Compartment Cell Model**
Białecki S, Kaźmierczak B[@]
Proceedings of the XX National Conference Applications of Mathematics in Biology and Medicine, Łochów, September 23-27,ISBN: 978-83-932893-1-8, pp. 15-20, (2014)

B **Stationary Waves on the Sphere**
Białecki S[⋆], Kaźmierczak B[@,⋆], Tsai J-C
SIAM J. APPL. MATH., **75**, *4, 1761-1788* (2015) Impact Factor 2015: 1.428

C **Regularity of solutions to a reaction-diffusion equation on the sphere: the Legendre series approach**
Białecki S, Kazmierczak B[@], Nowicka D, Tsai J-C
MATHEMATICAL METHODS IN THE APPLIED SCIENCES **40**, 14, 5349-5369 (2017)
Impact Factor 2017: 0.918

D **Polarization of concave domains by traveling wave pinning**
Białecki S, Kaźmierczak B., Lipniacki T[@]
PLOS ONE **12**, 12, e0190372-1-10 (2017) Impact Factor 2017: 2.806

E **The propagation phenomenon of solutions of a parabolic problem on the sphere**
Kaźmierczak B[@], Tsai J-C, Białecki S
Mathematical Models and Methods in the Applied Sciences **28**, 10, 2001-2067 (2018)
Impact Factor 2018: 2.860

F **Traveling and standing fronts on curved surfaces**
Białecki S, Nałęcz-Jawecki P, Kaźmierczak B, Lipniacki T[@]
Physica D **401**, 132215 (2020) Impact Factor 2018: 1.810

Full-text articles along with supplementary materials are provided in Section 8.
Signed declarations of author contributions are provided in Section 9.
Impact Factors are given for the year of publication according to the Journal Citation Reports. For recent publications, the latest available values are given.

[⋆] Co-first authors.
[@] Corresponding author.

The author of this thesis has authored or co-authored several other original research articles *not* included in the thesis:

- **Lie-Backlund Transformations and Gravitational Instantons**
  Przanowski M, Białecki S
  Acta Physica Polonica **B18**, 10, 879-889 (1987)

- **Zermelo's Theorem**
  Nowak B*, Białecki S* *Formalized Mathematics* **1**, 3, 431-432 (1990)

- **Photogeneration and photovoltaic effect in blends of derivatives of hexabenzocoronene and perylene**
  Jung J, Rybak A, Ślązak A, Białecki S, Miśkiewicz P, Głowacki I, Ulański J, Rosselli S, Yasuda A, Nelles G, Tomović Ž, Watson MD, Müllen K,
  Synthetic Metals **155**, 150-156 (2005)

1 Dynamics of free calcium ions inside eukariotic cell - paper A

Calcium Oscillations in a Spatially Extended Three Compartment Cell Model
Białecki S, Kaźmierczak B
Proceedings of the XX National Conference Applications of Mathematics in Biology and Medicine, Łochów, September 23-27,ISBN: 978-83-932893-1-8, pp. 15-20, (2014)

1.1 Motivation

The role of calcium in cell physiology is so fundamental that cannot be overestimated. The spatio-temporal distribution of calcium ions control diverse processes, such as *fertilization, proliferation, morphogenetic development, gene expression, learning and memory, synaptic communication, muscle contraction, hormone secretion, cell movement, wound repair and many, many more.* Appropriate level calcium in the cell must be ensured to generate sufficient amount of energy in the form of ATP which is a necessary condition to sustain life. Additionally, calcium is an universal carrier of biological signals[1],[2].

Calcium is one of the most important second messengers. This means that calcium ions relay signals received at receptors on the cell surface (binding of protein hormones, growth factors, etc.) to target molecules in the cytosol or nucleus, amplifying the strength of the signal and initiating appropriate regulatory pathways. In this way, the external signals (such as ligand to receptor binding) are trans-coded into increase of internal calcium ions concentration in the cytosol of the cell.

Moreover, the distribution of calcium concentration in the eukariotic cell compartments is not constatnt in time.

Thus there are continuous oscillations of Ca^{2+} concentration caused by flows of calcium ions between the cytosol and its intracellular stores: endoplasmic reticulum and mitochondria. In the case of vertebrates, it is estimated that around 20 percent of organism energy is used for maintaining these oscillations.

These temporary changes of calcium ions concentration are important, because high level of free calcium ions concentration is extremely harmful to the cell, so after fulfilling its role it must, as quickly as possible, be hidden back into internal reservoirs (the endoplasmic reticulum and mitochondria), where concentration of Ca^{2+} may be from 2 to 4 orders of magnitude higher with respect to the cytosol.

Generally, the signal transduction by calcium ions can be realized in two ways:

1. By initiation of appropriate regulatory pathways - through binding to relevant molecules calcium ions can cause rebuilding their conformation and thus change their state to active (see Figure 1),

2. By responding to appropriate mechanical strains. This, due to mechanochemical coupling, is a basic mechanism of many biological phenomena such as heart contraction and bacterial movement.

The starting point in my study of the phenomena of inter-compartmental flow of calcium ions and oscillations of their concentration in eukaryotic cells was the existing Marhl's model [3]. It was later modified in Michał Dyzma's doctoral dissertation [4] to take into account Mitochondria-Associated endoplasmic reticulum Membranes, known in the literature under the acronym MAMs. (See also [5], [6].) Both of the above mentioned ODE models describe the dynamics of calcium and buffer molecules concentrations averaged over the cell compartments. Such an approach can be justified by assuming relatively large diffusion coefficients of free calcium ions in all the considered compartments.

[1] Carafoli, E. Calcium - A universal carrier of biological signals. *The FEBS journal* **272,** 1073–89. doi:10.1111/j.1742-4658.2005.04546.x (Apr. 2005).

[2] Carafoli, E. & Krebs, J. Why Calcium? How Calcium Became the Best Communicator. *THE JOURNAL OF BIOLOGICAL CHEMISTRY* **291,** 20849–20857. doi:10.1074/jbc.R116.735894 (40 Sept. 2016).

[3] Marhl, M. *et al.* Complex calcium oscillations and the role of mitochondria and cytosolic proteins. *Biosystems* **57,** 75–86 (2000).

[4] Dyzma, M. *Modelowanie oscylacji stężeń jonów wapniowych w komórkach eukariotycznych z uwzględnieniem obszarów bezpośredniego kontaktu pomiędzy mitochondriami a retikulum endoplazmatycznym.* PhD thesis (IPPT PAN, 1st Nov. 2014).

[5] Morciano, G. *et al.* Role of mitochondria-associated ER membranes in calcium regulation in cancer-specific settings. *Neoplasia* **20,** 510–523 (2018).

[6] Yang, X. *et al.* Mitochondria-associated endoplasmic reticulum membrane: Overview and inextricable link with cancer. *Journal of cellular and molecular medicine* **27.** doi:10.1111/jcmm.17696 (Feb. 2023).

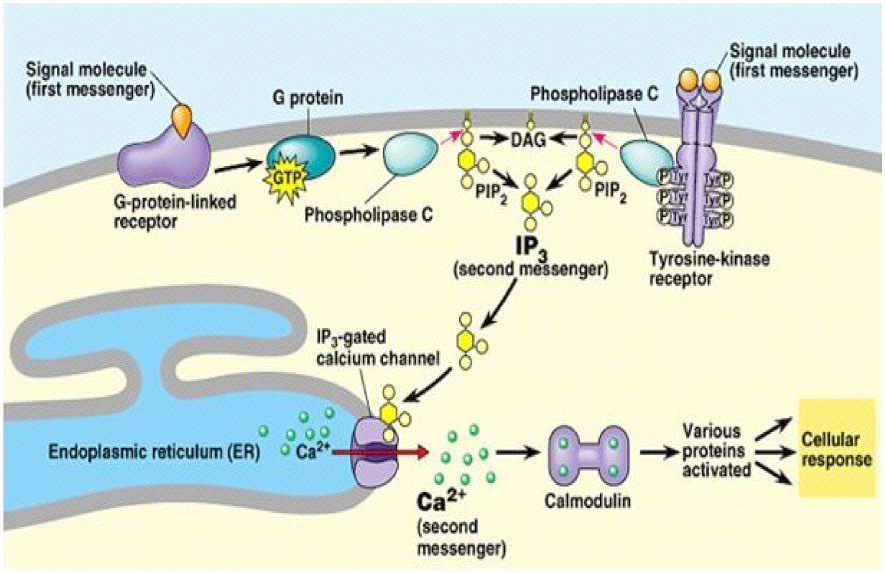

Figure 1: Calcium signaling in eucariotic cell

1.2 Main results of paper A

The natural question arises:
In what way the lower values of diffusion coefficients of calcium ions affect the existence and properties of oscillatory solutions for the spatially extended model?

To study this problem, we first designed the spatial extension of the Marhl's model by assuming a specific distribution of calcium reservoirs in the cytosol. Both the approximate shapes of the reservoirs, as well as their spatial configuration corresponded qualitatively to experimentally obtained images of these organella. The complicated geometry of the assumed distribution of the calcium vesicles made the numerical calculations of the initial boundary value problems extremely time consuming. To reduce this time, we resigned from the full generality of the possible three dimensional spatial configurations, and confined ourselves to the axisymmetric distributions of the compartments inside a spherical cell. We hope that this simplification had no influence on the qualitative validity of the obtained results. One of the basic conclusion of our numerical analysis was the observation that for typical biological cells and for diffusion coefficients of calcium ions from the physiologically accepted range, at a given moment of time, the spatial variability of calcium concentration in all of the compartments is negligible. This result is shown in Figure 2.

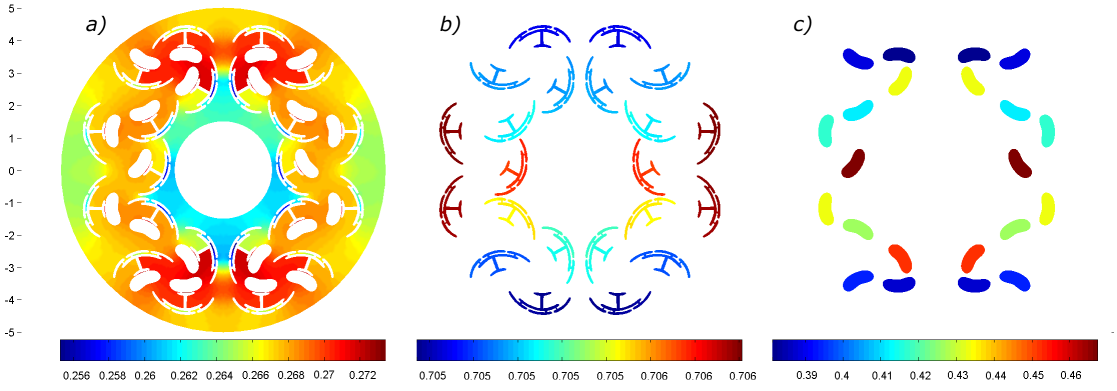

Figure 2: Example distributions of calcium ion concentrations at the same moment of time at the 2D cross-sections of the 3-dimensional ball with axially symmetric geometry of compartments modeling the biological cell. Colours show the calculated distributions of calcium concentration for: a) cytosol, b) reticulum and c) mitochondria. The radius of the cell and and diffusion coefficient of calcium ions are equal respectivelly to $5\mu m$ and $100\mu m^2/s$. The diffusion coefficient of buffers in the cytosol is equal to $1\mu m^2/s$.

The first task I undertook in my research was to construct a spatial model as a system of partial

reaction-diffusion equations describing the flow of calcium ions between intracellular calcium stores and the cytosol, consistent, in terms of the size of inter-compartmental flows, with the spatially homogeneous model of Marhl [7]. The derivation of the spatially extended model has been carried out by postulating a reaction diffusion system of equations in the compartments supplemented with no-flux boundary conditions at the outer boundary of the cell and nonlinear Robin boundary conditions at the interfaces of the inner compartments. The unknown coefficient functions were chosen via integration over the compartments volumes, applying Gauss-Ostrogradski theorem, and comparing the results with the equations of the spatialy homogeneous model. The additional conditions used in the construction of the model assumed that the buffers in reticular and mitochondrial compartments are 'fast' and the total amount of buffers is sufficiently large. (Precise formulation of these conditions are given after system (17)-(18) in **A**.)

The designed PDE model was used to check numerically the robustness of oscillatory solutions with respect to changes of diffusion coefficient of calcium ions, which has been assumed to be the same in all the compartments. To speed up calculations, effective diffusion for calcium ions was used for Mit and Ret compartments. For sufficiently large diffusion coefficients of calcium ions in the compartments ($\gtrsim 100\mu m^2/s$), the model exhibits oscillatory solutions very similar in their structure and period to the solutions observed in Marhl's model, i.e. relatively regular peak oscillations (as in the left upper panel of Figure 2 in **A**) of period equal to circa 10s. For decreasing values of the diffusion coefficient of calcium ions (assumed to be the same in all the compartments), this simple structure becomes more complicated. Groups of irregular high peaks are more and more separated by smaller ones until the oscillatory solutions cease to exist at $D_{cCyt} = D_{cMitt} = D_{cRet} = 13.5\,\mu m^2/s$. These results are presented at Figure 2 in **A**.

Numerical results were obtained via simulations by means of COMSOL Multiphysics software.

Finally, it is worth emphasizing that mitochondria and the endoplasmic reticulum have very complex geometry that is difficult to reproduce in the model. In particular, there are still many questions concerning the structure of the endoplasmic reticulum, which is a serious obstacle in designing more accurate models.

The problem of convergence of parabolic systems of equations on domains separated by semi-permeable membranes, when diffusion coefficients tend to infinity while the flux through the membranes remains constant, has been considered in the paper[8] One of the motivation of this analysis was the phenomenon of calcium flow between the calcium stores described above.

[7] Marhl, M. *et al.* Complex calcium oscillations and the role of mitochondria and cytosolic proteins. *Biosystems* **57,** 75–86 (2000).

[8] Bobrowski, A., Kazmierczak, B. & Kunze, M. An averaging principle for fast diffusions in domains separated by semi-permeable membranes. *Mathematical Models and Methods in Applied Sciences* **27** (Feb. 2016).

2 Reaction-diffusion waves on the sphere - papers B, C, E

2.1 Motivation and background

As we noted in the previous subsection, the space-time evolution of calcium ions plays a very important role in the physiology of eukaryotic cells. To date, very few aspects of the influence of calcium dynamics on the initiation and evolution even of the most significant cell signaling pathways have been explored. There is no doubt, however, that calcium is one of the most important information transmitters between individual organelles (compartments) of the cell, as well as between the intercellular space and the interior of the cell (in particular the nucleus). In long biological cells (e.g. in muscle cells) or in epithelial cells, the above-mentioned transfer of information may take place as a result of propagation of traveling waves of calcium concentration in the cytosol. In the mathematical description, such waves are often approximated by plane waves, for example as waves moving inside rectilinear cylindrical regions of constant cross-section with homogeneous Neumann boundary conditions (see, e.g. the book of Volperts[9]), The plane waves are relatively well known, both in the context of the proofs of their existence as well as their properties. These issues are discussed comprehensively in the Volperts' books[9] and, in the narrower range of calcium waves, in the book of Keener and Sneyd[10]. Propagation of calcium waves may, however, take place in more complex geometries as for instance on the curved surfaces corresponding to the cell membrane. The most spectacular example of such waves are calcium waves formed on the surface of the fertilized oocyte (see Figure 3). First observations of such traveling calcium waves on Medaka egg cells' membrane were made by Jaffe[11] in 1977.

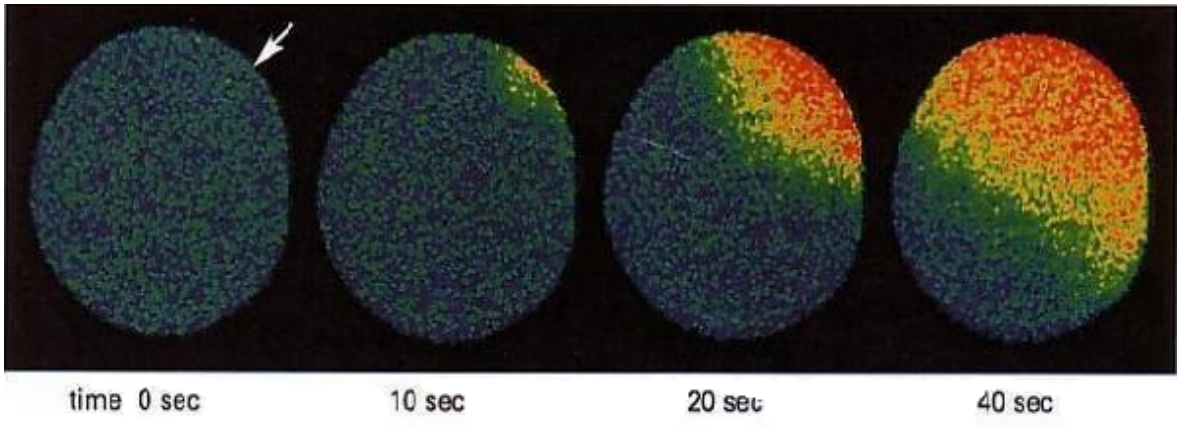

Figure 3: *Calcium wave just after fertilization on the surface of Medaka egg (Discovered and first visualized by Jaffe in 1978).*

From a mathematical point of view, such waves are much more interesting than plane waves and their description is more complex due to the fact that they move on curved surfaces. Moreover, non-zero curvature of the surface can often be a source of phenomena that have no counterparts for plane waves. This is a subject of papers D and F. Despite the fact that calcium waves are a kind of paradigm for traveling waves in biology, signal transduction phenomena can also be performed by traveling waves in which calcium ions play no role, such as receptor activation waves on the membranes of the immune cells of type B. Such waves have been studied, e.g. in paper[12] , where a mathematical model of the activation process based on an interaction of volume kinase molecules with membrane receptors has been proposed. The model is described by the following system of equations:

$$\begin{aligned} \frac{\partial K}{\partial t} &= D\nabla_S^2 K + a\,R\,(1-K) - \frac{b\,H\,K}{H+K} \\ \frac{\partial R}{\partial t} &= \gamma[(c_0+K^2)(P-R)-R]. \end{aligned} \tag{1}$$

where K is concentration of the active membrane kinase molecules, R - concentration of the activated receptors, a, b, H, c_0, γ - positive constants, D - surface diffusion of kinase molecules, P - uniform total

[9]Volpert, A. I., Volpert, V. A. & Volpert, V. A. *Traveling Wave Solutions of Parabolic Systems* (American Mathematical Society, 1994).

[10]Keener, J. & Sneyd, J. *Mathematical Physiology I* doi:10.1007/978-0-387-75847-3 (Springer New York, 2009).

[11]Ridgway, E. B., Gilkey, J. C. & Jaffe, L. F. Free calcium increases explosively in activating medaka eggs. *Proceedings of the National Academy of Sciences* **74,** 623–627. doi:10.1073/pnas.74.2.623 (Feb. 1977).

[12]Hat, B., Kaźmierczak, B. & Lipniacki, T. B cell activation triggered by the formation of the small receptor cluster: a computational study. *PLoS Computational Biology* **7,** e1002197. doi:10.1371/journal.pcbi.1002197 (10 Oct. 2011).

concentration of all receptors both the activated and inactivated ones.

Because $\frac{\partial R}{\partial t}$ is close to zero, then if we assume it to be equal to zero we can compute $R(K)$ from the second equation, after substitution to the first one, we obtain the following simplification of the model:

$$\begin{aligned} \frac{\partial K}{\partial t} &= D\nabla_S^2 K + \Phi(K) := \\ & D\nabla_S^2 K + aR(K)\cdot(1-K) - \frac{bHK}{H+K} \end{aligned} \tag{2}$$

For the parameters a, b, P, and H taken from physiological ranges , the reaction term $\Phi(K)$ is of bistable type in Hat[9]. By approximating the source by piecewise linear term $F(u,\sigma)$ in the McKean form (4) (see Figure 4) we arrive, after appropriate rescaling of time and space units, at the reaction-diffusion equation on the sphere:

$$\frac{\partial u}{\partial t} = \nabla_S^2 u + F(u,\sigma) \tag{3}$$

$$F(u,\sigma) = -Bu + B * H(u-\sigma) \tag{4}$$

where B and σ are positive constants, and ∇_S^2 is a Laplace-Beltrami operator on the sphere, i.e.

$$\nabla_S^2 := \frac{1}{\sin x}\frac{\partial}{\partial x}(\sin x \frac{\partial}{\partial x}) = \frac{\partial^2}{\partial x^2} + \cot x \frac{\partial}{\partial x}. \tag{5}$$

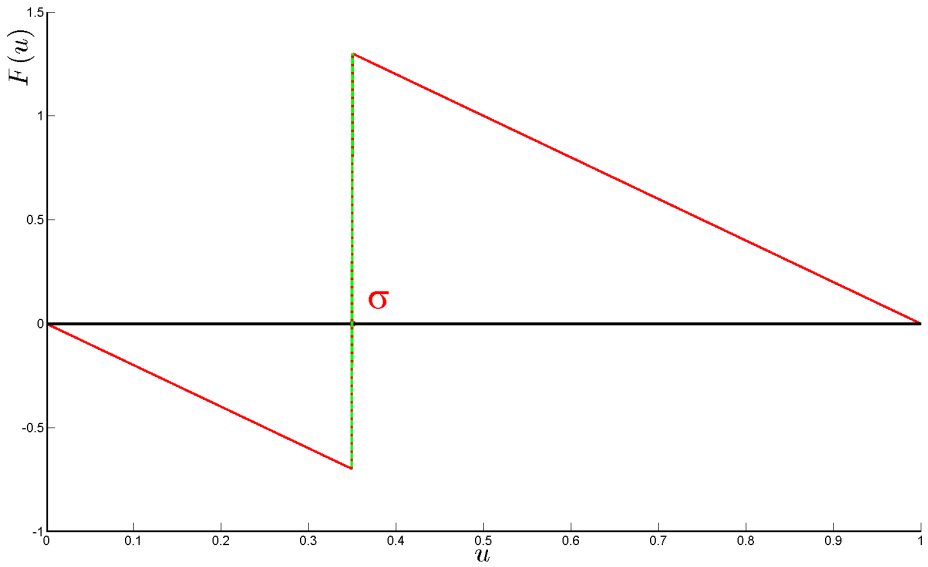

Figure 4: The assumed McKean form of $F(u,\sigma)$

$H(\cdot)$ is the Heaviside function: $H(v) = 1$ for $v > 0$, $H(v) = 0$ for $v < 0$ and $H(0) = H_M \in [0,1]$.

In axisymmetric case problem (3) reads:

$$\frac{\partial u}{\partial t} = \frac{1}{\sin x}\frac{\partial}{\partial x}\left(\sin x \frac{\partial u}{\partial x}\right) + F(u,\sigma) \tag{6}$$

where $(x,t) \in (0,\pi)\times(0,T]$ and F is given by (4), subject to the boundary conditions

$$u_{,x}(0,t) = u_{,x}(\pi,t) = 0, \tag{7}$$

and initial conditions

$$u(0,x) = u_0(x). \tag{8}$$

We are interested in solutions $u(x,t)$ with negative x-derivative, i.e. such that

$$\frac{\partial u}{\partial x}(x,t) < 0, \quad \text{for} \quad (x,t) \in (0,\pi)\times[0,T).$$

Let ${}_2F_1(a,b,c;z)$ denote the (Gaussian) hypergeometric function satisfying the hypergeometric equation

$$z(1-z)\frac{d^2w}{dz^2}+[c-(a+b+1)z]\,\frac{dw}{dz}-abw=0 \tag{9}$$

where $a,b,c\in\mathbb{R}$.
If $\lambda_B=\frac{1}{2}\cdot\big(-1+\sqrt{1-4B}\big)$ (and $-\lambda_B\cdot(\lambda_B+1)=B:=a\cdot b$), then ${}_2F_1(-\lambda_B,\lambda_B+1,1;z)$ satisfies the equation

$$\Big(z(1-z){}_2F_1(-\lambda_B,\lambda_B+1,1;z)_{,z}\Big)_{,z}-B\ {}_2F_1(-\lambda_B,\lambda_B+1,1;z)=0, \tag{10}$$

hence the equation

$$\begin{aligned}&\Big[{}_2F_1(-\lambda_B,\lambda_B+1,1;\tfrac{1-\cos x}{2})\Big]_{,xx}-\cot x\ \Big[{}_2F_1(-\lambda_B,\lambda_B+1,1;\tfrac{1-\cos x}{2})\Big]_{,x}\\&-B\ {}_2F_1(-\lambda_B,\lambda_B+1,1;\tfrac{1-\cos x}{2})=0.\end{aligned} \tag{11}$$

Remark 1
In the model, the discontinuity of the source function in the point $u=\sigma$ implies the discontinuity of the second derivative of the stationary solution to system (6)-(7) at a point $x=\eta_0$. It is crucial that there exists a bijective correspondence between $\sigma\in[0,1]$ and $\eta_0\in[0,\pi]$. This correspondence is very helpful in constructing solutions to the considered system. □

The properties of stationary solutions to the boundary value problem (6)-(7) can be summarized in the following lemma.

Lemma 1 *(THEOREM 2.1 in paper* **[B]** *and Lemma 5.1 in paper* **[E]**)
Given $\sigma\in(0,1)$ and $B>0$, we can find a unique $\eta_0\in(0,\pi)$ such that the function

$$U(x;\eta_0)=\begin{cases}1+C_1(\eta_0)\cdot{}_2F_1(-\lambda_B,\lambda_B+1,1;\frac{1-\cos x}{2}), & 0<x<\eta_0,\\ C_2(\eta_0)\cdot{}_2F_1(-\lambda_B,\lambda_B+1,1;\frac{1+\cos x}{2}), & \eta_0<x<\pi,\\ \sigma, & x=\eta_0,\end{cases} \tag{12}$$

satisfies the equations

$$\frac{1}{\sin x}\frac{\partial}{\partial x}\left(\sin x\frac{\partial U}{\partial x}\right)+B-Bu=0,\quad \text{for}\ \ 0<x<\eta_0, \tag{13}$$

$$\frac{1}{\sin x}\frac{\partial}{\partial x}\left(\sin x\frac{\partial U}{\partial x}\right)-Bu=0,\qquad \text{for}\ \ \eta_0<x<\pi, \tag{14}$$

and the boundary conditions

$$\frac{\partial U}{\partial x}(0;\eta_0)=\frac{\partial U}{\partial x}(\pi;\eta_0)=0. \tag{15}$$

Here, $C_1(\eta_0)\in(-1,0)$ and $C_2(\eta_0)\in(0,1)$ are given by the expressions:

$$\begin{aligned}C_1(\eta_0)&=C_1(\eta_0;B)=-\tfrac{1}{c_W}\ {}_2F_1(-\lambda_B+1,\lambda_B+2,2;\tfrac{1+\cos\,\eta_0}{2})\tfrac{\sin^2\eta_0}{2},\\ C_2(\eta_0)&=C_2(\eta_0;B)=\tfrac{1}{c_W}\ {}_2F_1(-\lambda_B+1,\lambda_B+2,2;\tfrac{1-\cos\,\eta_0}{2})\tfrac{\sin^2\eta_0}{2},\end{aligned} \tag{16}$$

where, for $\lambda_B=\frac{1}{2}\cdot\big(-1+\sqrt{1-4B}\big)$ and $S=4B-1$,

$$c_W=\frac{2}{\Gamma(-\lambda_B+1)\Gamma(\lambda_B+2)}=8\Big(\pi(S+1)sech\Big(\frac{\pi\sqrt{S}}{2}\Big)\Big)^{-1} \tag{17}$$

The function $U(x;\eta_0)$ defined by (12) is of class $C^1_x([0,\pi])\cap C^2_x([0,\eta_0))\cap C^2_x((\eta_0,\pi])$, monotonically decreasing on $(0,\pi)$, and satisfies

$$1>U(0;\eta_0)>U(x;\eta_0)>U(\pi;\eta_0)>0$$

for $x\in(0,\pi)$. Finally, we have that the map

$$\eta_0\in(0,\pi)\longmapsto\sigma=\sigma(\eta_0):=U(\eta_0;\eta_0)\in(0,1) \tag{18}$$

is of C^1-class, increasing, bijective, and $\frac{dU(\eta_0;\eta_0)}{d\eta_0}=\frac{d\sigma}{d\eta_0}>0$ for all $\eta_0\in(0,\pi)$. Moreover, for $0<a<b<\pi$, $\sigma(\cdot)\to1/2$ uniformly on $[a,b]$ as $B\to\infty$.

2.2 Main results of the paper [B]

Stationary Waves on the Sphere
Białecki S, Kaźmierczak B, Tsai J-C
SIAM J. APPL. MATH., **75**, *4, 1761-1788*

In paper [B] due to the adopted assumption on the source term in the McKean form, the stationary counterpart of Eq. (3) have been solved analytically. The solution is constructed by means of sewing the partial solutions corresponding to the linear parts of the function $F(u,\sigma)$ (shown in Figure 4) in the C^1 class. The sewing procedure is carried out at the appropriate point $x = \eta_0(\sigma) \in [0,\pi]$ such that $U(\eta_0(\sigma);\eta_0(\sigma)) = \sigma$. In this way, we can obtain a solution to Eq. (3) which belongs to the class $C^{1,1}([0,\pi])$, and to the class $C^1_x([0,\pi]) \cap C^2_x([0,\eta_0(\sigma))) \cap C^2_x((\eta_0(\sigma),\pi])$ (see THEOREM 2.1 in the paper [B]). The sewing point $\eta_0(\sigma)$ is uniquely defined. Moreover, according to THEOREM 2.5 the mapping $(0,\pi) \ni \eta_0 \mapsto U(\eta_0;\eta_0) = \sigma \in (0,1)$ is bijective (see Figure 5 where the dependence σ on η is visualised).

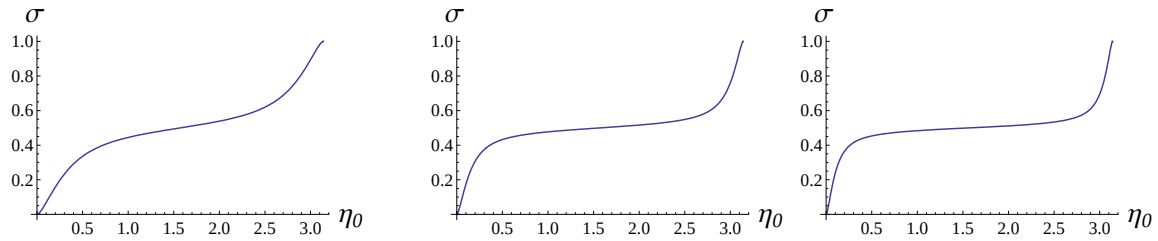

Figure 5: *Relation between between the transition (sewing) point η_0 and the parameter σ for B= 10, 50 and 100.*

This analytical form of solution facilitates significantly mathematical analysis of the wave front propagation on the sphere. In particular, we were able to explain the phenomena of activation fronts on the sphere that were examined numerically in[12] .

Though the constructed stationary wave is unstable (see, THEOREM 4.1, p.1778 in [B]), it has a very important property as a separatrix between the two sets of initial data. The initial data from the first set generate solutions tending to the inactive state ($u \equiv 0$), while the elements of the other one evolve to the active state ($u \equiv 1$).

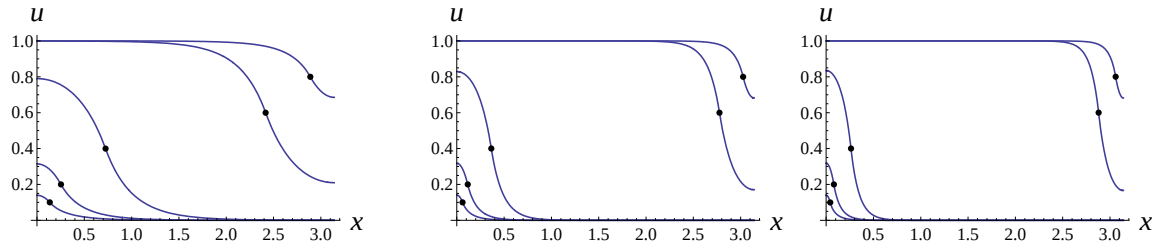

Figure 6: *Profiles of the standing fronts (separatrices) for different values of σ: 0.1 (the lowest curves), 0.2, 0.4, 0.6, 0.8 (the highest curves) for different values of B: 10 (left panel), 50 (middle panel) and 100 (right panel). By dots we have denoted the points $(\eta(\sigma),\sigma)$.*

Thus the constructed stationary wave can be treated as a threshold condition for the immune cell activation. In a way, it determines the minimal activation, which can induce the propagation of the activation wave. As it follows from Figure 6, the smaller the value of σ, the smaller portion of receptors should be stimulated to initiate the activation wave. Moreover, for large values of the parameter B which, via scaling, corresponds to low values of diffusion coefficient, we can observe very high sensitivity of the separatrix location with respect to the parameter σ. It changes very strongly with the parameter σ in the vicinity of $\sigma = 0.5$. Biologically, this can be interpreted as the possibility of cell activation in the aftermath of a small internal reorganization of the cell which can be sufficient for appropriate (though small) changes of the parameter σ. The Figure 7 below presents the example profiles of two separatrices for change of σ from $\sigma = 0.48$ to $\sigma = 0.52$ ($B = 1000$).

[12]Hat, B., Kaźmierczak, B. & Lipniacki, T. B cell activation triggered by the formation of the small receptor cluster: a computational study. *PLoS Computational Biology* **7,** e1002197. doi:10.1371/journal.pcbi.1002197 (10 Oct. 2011).

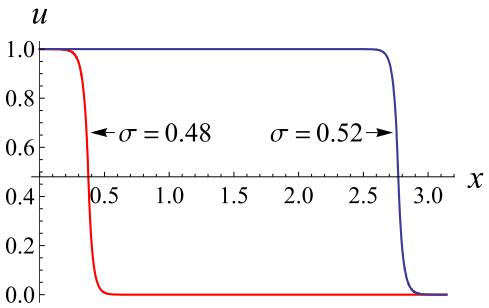

Figure 7: *The profiles of the stationary solutions $U_0(x;\sigma_0)$ to system (3-4) with $B = 1000$ for $\sigma = 0.48$ and $\sigma = 0.52$. The coordinate x denotes the zenith angle.*

2.3 Main results of the paper C

Regularity of solutions to a reaction-diffusion equation on the sphere: the Legendre series approach

Białecki S, Kazmierczak B, Nowicka D, Tsai J-C

MATHEMATICAL METHODS IN THE APPLIED SCIENCES **40**, 14, 5349-5369 (2017)

This work examines the regularity of solutions to the equation

$$\frac{\partial u}{\partial t} = D\nabla_S^2 u + F(u;\sigma), \tag{19}$$

where ∇_S^2 is the Laplace-Beltrami operator defined by (5). $F(u;\sigma)$ is a piecewise linear function imitating a bistable function:

$$F(u;\sigma) = -Bu + BH(u-\sigma), \tag{20}$$

where B and $\sigma \in (0,1)$ are positive constants and $H(\cdot)$ is the Heaviside function (see Figure 4). According to the assumed symmetry of the problem, Eq.(19) is supplemented with homogeneous boundary conditions of the Neumann type for $x = 0, \pi$. As we are interested in time dependent solutions to (19), we must also specify the initial condition $u(x,0) = u_0(x)$. In this work, we examined the properties of solutions to Eq.(19). Such solutions can describe the dynamics of many signaling phenomena on the membrane of biological cells. Although in this paper we have not studied yet the existence of solutions, we have been able to characterize their properties, mainly in terms of regularity, what may be considered as an initial step in the analysis of the existence of time dependent solutions. (Similar investigation has been carried out in an augmented form in paper E.) In particular, we were able to prove that if the 'mild solution' of Eq.(19), i.e. the solution of the integral equation

$$u(x,t) = \int_0^\pi G(x,y,t)u_0(y)\sin y\, dy + \int_0^t\int_0^\pi G(x,y,t-s)F(u(y,s);\sigma)\sin y\, dyds, \tag{21}$$

where

$$G(x,y,t-s) = \sum\nolimits_{l=0}^{l=\infty} \exp(-l(l+1)(t-s))P_l(\cos x)P_l(\cos y), \tag{22}$$

belongs to the class

$$C^0([0,T], L^2((0,\pi))) \cap BV([0,\pi]\times[0,T]),$$

then it also belongs to the class

$$C^{1,\beta}_{x,t}([0,\pi]\times[0,T])$$

for all $\beta \in (0,1/4)$ and satisfies the Neumann type boundary conditions $u_{,x}(0,t) = u_{,x}(0,t) = 0$ for all $t \in [0,T]$.

To prove this fact, we assumed that

$$u_0 \in C^4([0,\pi]); \quad u_{0,x}(0) = u_{0,x}(\pi) = 0; \quad u_{0,xxx}(0) = u_{0,xxx}(\pi) = 0 \tag{23}$$

and the mild solution $u(x,t)$ is such that the function

$$f(\cdot,t) := F(u(\cdot,t),\sigma)$$

belongs to the space of functions of bounded variation $BV([0,\pi])$ and is continuous at the ends of the interval $[0,\pi]$, i.e.

$$f(\cdot,t) \in BV([0,\pi]) \cap (C([0,\iota]) \cap C([\pi-\iota,\pi])) \qquad for \quad some \quad \iota \in (0,\pi). \tag{24}$$

We also assumed that the Legendre coefficients $w_l(f,t)$ (defined in (27)) behave in such a way that:

$$|w_l(f(\cdot,t))| \leq \frac{1}{\sqrt{l}} g(l;t) \tag{25}$$

for fome function $g(l;t) \to 0$ as $l \to \infty$, uniformly with respect to $t \in [0,T]$.

The proof is based on the analysis of the absolute convergence of the expansion of the function u into a series of Legendre polynomials with time-dependent coefficients:

$$\begin{aligned} &u(x,t) = \textstyle\sum_{l=0}^{l=\infty} \exp(-l(l+1)t) P_l(\cos x) w_l(u_0) \\ &+ \textstyle\sum_{l=0}^{l=\infty} P_l(\cos x) \int_0^t \exp(-l(l+1)(t-s)) \Big[\int_0^\pi P_l(\cos\xi) F(u(\xi,s);\sigma) \sin\xi \, d\xi \Big] ds, \end{aligned} \tag{26}$$

where

$$w_l(u_0) := \int_0^\pi P_l(\cos x) u_0(x) \sin x \, dx$$

denotes the l-th Legendre expansion coefficient of the initial data u_0. Similarly, for any function $f : [0,\pi] \times [0,T]$, $T > 0$, and any l, we denote by $w_l(f,t)$ its l-th Legendre coefficient, i.e

$$w_l(f,t) := \int_0^\pi P_l(\cos x) f(x,t) \sin x \, dx. \tag{27}$$

The results of the paper C provide a class of 'a priori' estimates that can be used in a proof of existence of solutions to Eq.(19), in particular by using sub- and super- solution methods.

The elliptic operator at the right-hand side of Eq. (5) has a singularity at $x = 0$ and $x = \pi$. However, because spheres are rotationally invariant, one can expect that solutions of Eq. (5) are regular (i.e., at least of $C^{2,1}_{x,t}$ class), at points where the source functions are smooth. This can be seen by an appropriate change of coordinates close to the points $x = 0$ and $x = \pi$ and using the bootstrap arguments. (For this kind of effective approach see Theorem 4.3 in E.) In the paper, however, we prove the x-differentiability (together with Hölder continuity with respect to time), by analyzing the convergence of the infinite series representation and its term-by-term differentiation for all $t \in (0,T)$. We think that this method of proof has a significance by itself, especially in the context of iterative methods. In the proof we use the results of paper[13], where the properties of solutions to the equation

$$Q_l'' + q_l(x) Q_l = 0,$$

with

$$q_l(x) = \nu^2 - \frac{3}{4 sin^2 x}, \quad \nu = \nu(l) = (l + \frac{1}{2})$$

were analysed.

The main difficulty (implied by the chosen method) is related to the necessity of accurate estimates of highly oscillating functions of the form

$$Q_l(x) = (1 - cos^2 x)^{3/4} \frac{dP_l(y)}{dy}|_{y=cosx}. \tag{28}$$

These estimates are necessary to show the convergenve of the infinite series S_{fB} defined by Eq.(29) in the paper C.

[13] Antonov, V. A., Kholshevnikov, K. V. & Shaidulin, V. S. Estimating the Derivative of the Legendre Polynomial. *Vestnik St. Petersburg University. Mathematics* **43,** 191–197. doi:10.3103/S1063454110040011 (4 Apr. 2010).

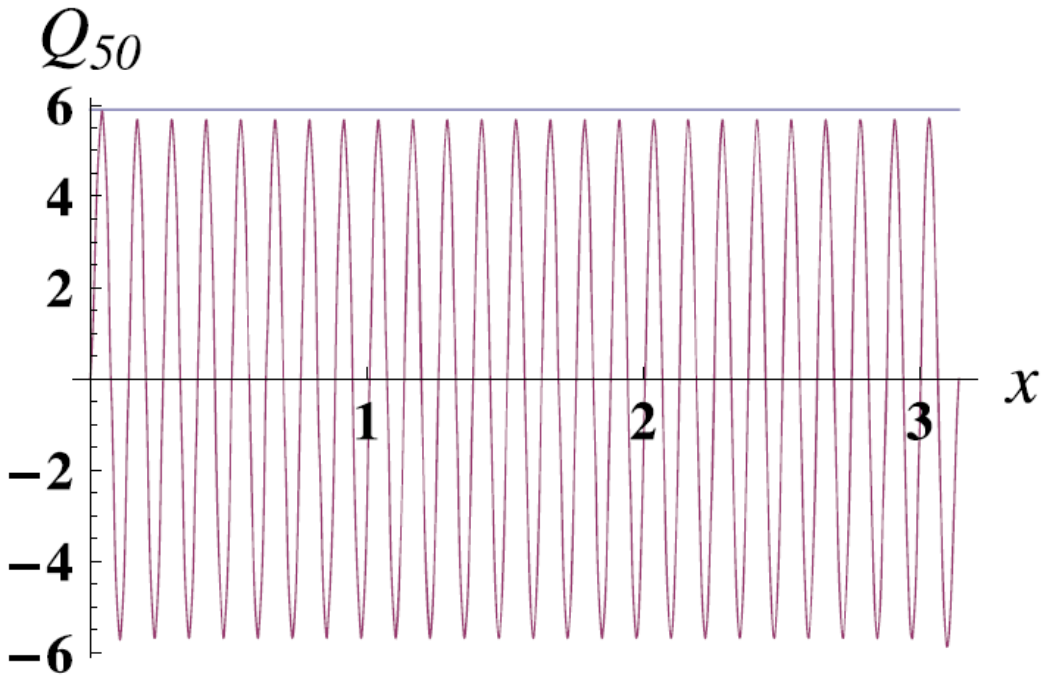

Figure 8: The graph of the function Q_{50} defined by (28).

2.4 Main results of the paper [E]

The propagation phenomenon of solutions of a parabolic problem on the sphere
Kaźmierczak B, Tsai J-C, Białecki S
Mathematical Models and Methods in the Applied Sciences **28**, 10, 2001-2067 (2018)

As in the previous work [C], here we analyze time dependent solutions to the equation

$$\frac{\partial u}{\partial t} = D\nabla_S^2 u + F(u;\sigma) \tag{29}$$

on the unit sphere S, where

$$F(u;\sigma) = -Bu + BH(u-\sigma), \tag{30}$$

$B > 0$ and $\sigma \in (0,1)$ subject to boundary conditions

$$u_x(x,t) = u_x(\pi,t) = 0, \tag{31}$$

and initial conditions

$$u(x,0) = u_0(x). \tag{32}$$

Continuing the analysis started in the paper [C], we focus on the problems of the existence of solutions having the form of a propagating front connecting states (places) of $u = 0$ and $u = 1$. Such an objective is motivated by the phenomenon of calcium wave propagation observed on the surface of large oocytes, or wave phenomena related to activation of receptors on the membrane of B cells.

In this work, we investigate existence and uniqueness of solutions of an integral equation associated with Eq. (29) and expressed formally by a series of Legendre polynomials with time dependent coefficients. Due to the assumed discontinuity of the reaction kinetics, standard methods of convergence analysis cannot be used for such series and their derivatives, i.e. series obtained by differentiation with respect to x. We would like to note that the choice of the above discontinuous source function is dictated by the fact that for this kind of function, we can find exact solutions for the stationary problem depending on the parameter σ. From these functions which are solutions to the stationary problem, we construct solutions for the time dependent problem, having in mind, in particular, solutions in the form of traveling fronts. By finding the appropriate a priori estimates for the expansion coefficients of the solution into a series of Legendre polynomials, we prove, using the method of sub- and super-solutions, the existence of the desired solution.

In particular, we prove that the constructed solutions are class $C^{2,1}_{x,t}$ everywhere away from the point $(x_\sigma(t), t)$, where $u(x_\sigma(t), t) = \sigma$ and σ is 'discontinuity point' of the source function $F(\cdot;\sigma)$.

The paper also includes the results of numerical simulations showing that the constructed sub- and super-solutions in fact constrain the actual solutions to the considered time dependent problem.

The core results of **Part I** of the paper [E] constist of three theorems about existence and smoothness of the solution to the problem (29) - (32) containing increasingly stronger results with the same two assumptions.
The first assumption concerns properties of the initial function u_0. The second assumes existence and properties of (mild) super- and sub-solution to problem (29).

First assumption: We assume that the function u_0 is $C^1([0,\pi])$, has first and third derivative equal zero at the ends of interval $(0,\pi)$, is a decreasing function, and 'disjointly' bounded in the class C^4.

This assumption (Assumption 4.1 p.2021) in the paper [E] is formally written as:

The function $u_0 \in C([0,\pi])$ *is such that*

$$\begin{aligned} &u_0 \in C^1([0,\pi]), \quad \textit{and} \quad ||u_0||_{C^4([0,a])} + ||u_0||_{C^4([a,\pi])} < \infty, \\ &u_{0,x}(0) = u_{0,x}(\pi) = 0, \quad \textit{and} \quad u_{0,xxx}(0) = u_{0,xxx}(\pi) = 0, \\ &\frac{\partial u_0(x)}{\partial x} < 0 \quad \textit{for} \quad \textit{all} \quad x \in (0,\pi). \end{aligned} \tag{33}$$

Second assumption: We assume that mild super-solution W and sub-solution V exist in class $C^{1+\alpha_0,\beta_0}_{x,t}([0,\pi]\times[0,T])$ for some $\alpha_0, \beta_0 \in (0,1)$. They both have their range in $(0,1)$ and are decreasing in x.

This assumption (Assumption 4.2 p.2022) in the paper [E] is formally written as:

There exist functions W, V of class $C^{1+\alpha_0,\beta_0}_{x,t}([0,\pi]\times[0,T])$ for some $\alpha_0, \beta_0 \in (0,1)$ which are respectively (mild) super- and sub-solution to problem (29), (30), (31), (32) and which satisfy

$$0 \le W(x,t) \le 1 \quad \textit{and} \quad 0 \le V(x,t) \le 1, \tag{34}$$

$$\frac{\partial W}{\partial x}(x,t) \le 0 \quad \textit{and} \quad \frac{\partial V}{\partial x}(x,t) \le 0 \tag{35}$$

for all $(x,t) \in (0,\pi)\times(0,T)$.
For each $t \in (0,T)$ each of the equations $W(\cdot,t) = \sigma$ and $V(\cdot,t) = \sigma$ has at most one solution.

Basing on this assumptions, we are able to prove the following theorems:

Theorem 4.1, p. 2023 . *There exist the maximal mild solution U (resp. the minimal mild solution u) to initial boundary value problem (29) - (32), which belongs to the class $C^{1+\alpha,\beta}_{x,t}([0,\pi]\times[0,T])$ for any $\alpha \in (0,1/2)$ and $\beta \in (0,1/4)$, is in the ordered interval $[V,W]$ of the sub-solution V and the super-solution W, and satisfies $U_x(\cdot,t) < 0$ on $(0,\pi)\times(0,T)$, (resp. $u_x(\cdot,t) < 0$ on $(0,\pi)\times(0,T)$).*
Theorem 4.2, p.2031. *There exists unique mild solution u to system (29) - (32) which belongs to the class $C^{1+\alpha_0,\beta_0}_{x,t}([0,\pi]\times[0,T])$ for some $\alpha_0, \beta_0 \in (0,1)$. The solution u is unique for all $t \in (0,T)$.*

Theorem 4.3, p.2033. *There exists unique mild solution u to the problem (29) - (32) which belongs to the class $C^{1+\alpha_0,\beta_0}_{x,t}([0,\pi]\times[0,T])$ for some $\alpha_0, \beta_0 \in (0,1)$. For each $t \in (0,T)$ there exist a unique point x_σ such that $u(x_\sigma(t),t) = \sigma$ and away from this point $u \in C^{2,1}_{x,t}$. The solution u is unique for all $t \in [0,T]$.*

In sections 5 and 6 in **Part II** of the paper [E] we continue considering propagating behaviour of solutions to system (29) - 32). To show the existence of wave like solutions propagating on the sphere according to **Theorem 4.3** we have to show the existence of the proper super- and sub-solutions required by second assumption. Section 5.1 contains construction of time dependent super-solution and section 5.2 - construction of time dependent sub-solution. In section 5.3 we prove that the solution to problem (29) - (32) during propagtion is lying between constructed sub- and super-solution. Section 5.4 provides concrete numerical examples of solutions, sub- and super-solutions, which were more generally considered in section 5.3 and presents them graphically (see Figure 9 and Figure 10 below).

In Discussion (section 6) we applied the results to the species with very small diffusivity. We showed that the assumption $B \gg 1$ used in section 5 is biologically justified. By scaling arguments we also showed that the speed of the obtained solutions corresponds to the experimental values for $B \approx 1000$.

Construction of time-dependent super-solution.
Let $U(x;\eta_0)$ be stationary solution defined in Eq.(12) to problem (6)-(7) in **Lemma 1**. The super-solution is sought in the form $U(x;\eta_0^+(t))$ with sufficiently chosen function $\eta_0^+(t) \in C^1[0,T^+]$ for some $T^+ > 0$:

$$\eta_0^+(0) = \eta_0^\sharp,\ \eta_0^+(T^+) = \tilde{\eta}_0,\ \text{ and } (\eta_0^+)'(\cdot) > 0 \text{ on } [0,T^+], \tag{36}$$

which satisfies the supersolution condition:

$$\frac{d\eta_0^+(t)}{dt} \cdot \frac{\partial U}{\partial \eta_0}(x;\eta_0^+(t)) \ge E(x;\eta_0^+(t)) \tag{37}$$

where

$$E(x;\eta_0^+(t)) = F(U(x;\eta_0^+(t)),\sigma_0) - F(U(x;\eta_0^+(t)),\sigma(\eta_0^+(t))). \tag{38}$$

A super-solution to the boundary value problem (29)-(32) in the limit of big B is given by the following theorem.

Theorem 5.1 p. 2048. *Let $\eta_0^\sharp \in (0,\pi/2)$ and $\tilde{\eta}_0 = \pi - \eta_0^\sharp \in (\pi/2,\pi)$. Then there exist constant $\underline{b}$ such that for all $B > 0$ sufficiently large, the function*

$$U^+(x;t) := U(x;\eta_0^+(t))$$

with

$$\eta_0^+(t) := 4\sqrt{B}\,\underline{b}^{-1}\,t + \eta_0^\sharp \tag{39}$$

is a super-solution of Eq. (6-7) for all $(x,t) \in [0,\pi] \times [0,T^+]$

where $T^+ := \dfrac{\tilde{\eta}_0 - \eta_0^\sharp}{4\underline{b}^{-1}\sqrt{B}}$.

Remark 2

The existence of $\underline{b}$ follows from Eqs.(5.31), (5.34), (5.35) in the paper. □

Construction of time-dependent sub-solution.

Lets begin with choosing $\hat{\eta}_0 \in (0,\pi/2)$ and set $\sigma_0 = \sigma(\hat{\eta}_0)$. Since σ as the function of η_0 is increasing in $(0,\pi)$ and $\sigma(\pi/2) = 1/2$ (see Eq. (18) and Lemma 1 or PROPOSITION 2.2 and PROPOSITION 2.3 p. 1767 of paper [B]).

$$\sigma_0 \in (0,1/2). \tag{40}$$

Let us also choose a parameter v with

$$v \in (0, 1/2 - \sigma_0). \tag{41}$$

The subsolution is sought in the form $U(x;\eta_0^-(t),v)$ where:

$$U(x;\eta_0^-,v) := U(x;\eta_0^- + k_v(\eta_0^-)) - v \tag{42}$$

with $k_v(\eta_0^-)$ defined as satisfying the condition

$$\sigma(\eta_0^- + k_v(\eta_0^-)) = \sigma(\eta_0^-) + v \;\; \left(= U\left(\eta_0^- + k_v(\eta_0^-); \eta_0^- + k_v(\eta_0^-)\right)\right. \tag{43}$$

Let

$$\Gamma(\eta_0^-) = \Gamma(\eta_0^-; v, B) := \frac{d\sigma}{d\eta_0}(\eta_0^-)\left(\frac{d\sigma}{d\eta_0}(\eta_0^- + k_v(\eta_0^-))\right)^{-1}. \tag{44}$$

Next, we fix $\chi > \dfrac{3}{2}$, and let the function $\eta_0^- : [0,T^-) \mapsto (0,\pi)$ be defined as the solution to an ordinary differential equation:

$$\frac{d\eta_0^-}{dt}(t) = \frac{v}{\Gamma(\eta_0^-(t))\chi} \cdot \sqrt{B}, \tag{45}$$

where T^- is such that:

$$\eta_0^-(T^-) = \tilde{\eta}_0 \quad \textit{and} \quad \sigma(\tilde{\eta}_0) = 1 - v. \tag{46}$$

We assume that η_0^- satisfies the initial condition:

$$\eta_0^-(0) = \hat{\eta}_0.$$

Where $\hat{\eta}_0, \tilde{\eta}_0$ were previously set.
The construction of the sub-solution $U^-(x,t)$ of Eq. (6) is summarized in the following theorem.

Theorem 5.2 p.2052 *For B sufficiently large, the function $U^-(x,t)$ given by*

$$U^-(x,t) = \begin{cases} U(x;\eta_0^-(t),v) & \textit{for } t \in [0,T^-), \\ 1 - v\cdot\exp(-B(t-T^-)) & \textit{for } t \in [T^-,\infty). \end{cases} \tag{47}$$

is a sub-solution of Eq. (6). Here $\eta_0^-(t)$ and T^- are defined by (45) and (46), respectively.

Numerical examples

The numerical simulations confirm that the actual solution to the considered time dependent problem is lying between the constructed sub- and super-solutions if only the initial solution is lying between the constructed initial sub- and initial super-solution as shown in Figures 9 and 10. In our numerical simulations, we take the following values of the parameters defining the super- and sub-solution to Eq. (6):

$$\begin{aligned} &B = 1000,\ \hat{\eta}_0 = \pi - 3.05,\ \sigma_0 = \sigma(\hat{\eta}_0) = 0.40876,\ v = 0.05, \\ &\chi = 5/3,\ \eta_0^\sharp = \hat{\eta}_0 + 0.2, \sigma(\eta_0^\sharp) = 0.47353. \end{aligned} \tag{48}$$

The initial position of the subsolution $U(\cdot;\hat{\eta}_0,v)$ is equal to $U(\cdot;\hat{\eta}_0{+}0.1){-}v$. It follows that $k_v(\hat{\eta}_0) \approx 0.1$ (where k_v is defined in (43)). From (48) and the increasing properties of $U(\cdot;\eta_0)$ with respect to $\eta_0 \in (0,\pi)$, we conclude that, in fact, $U(x;\hat{\eta}_0,v) < U(x;\eta_0^\sharp)$ for all $x \in [0,\pi]$.

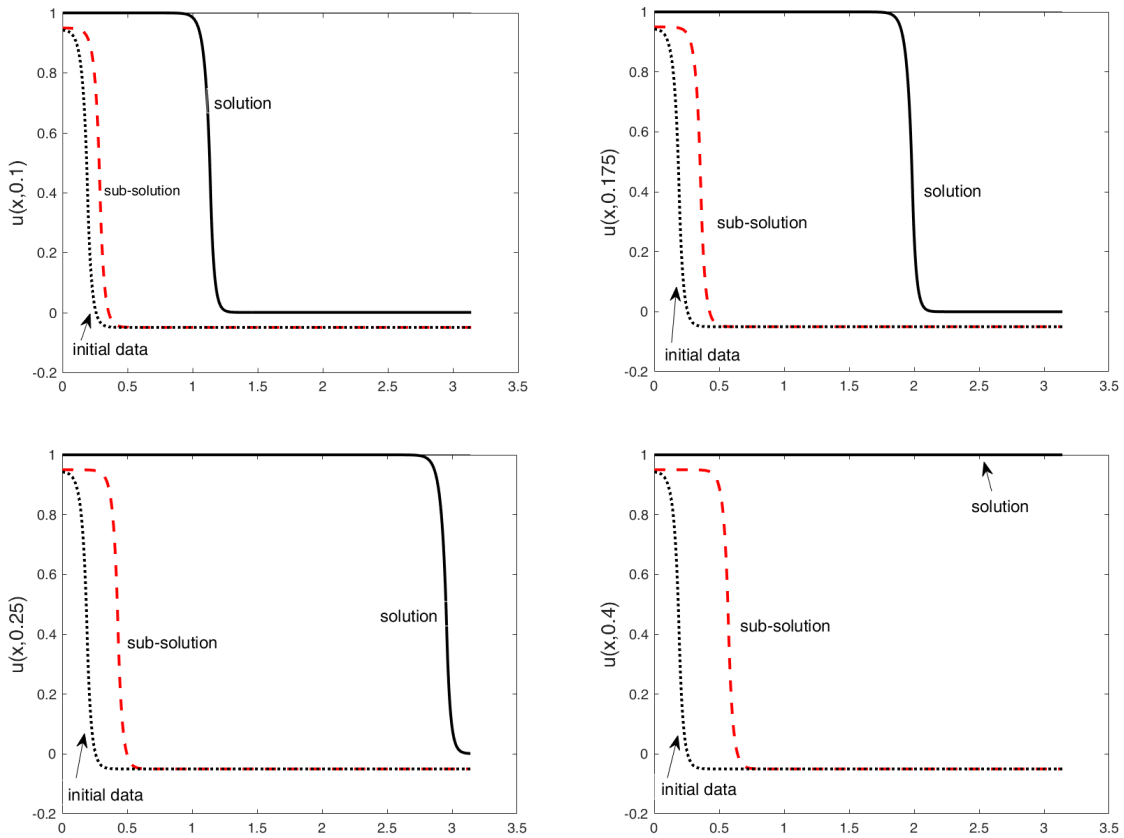

Figure 9: The dotted black curve corresonds to $U(x;\hat{\eta}_0,v)$, i.e. the initial sub-solution curve, and simultaneously the initial condition for Eq.(6). The solid black curves depict the solution to Eq.(6) and the dashed red curves correspond to the sub-solutions at the given time. Left upper panel: The sub-solution and solution curves for $t = 0.1$. Right upper panel: The sub-solution and solution curves for $t = 0.175$. Left lower panel: The sub-solution and solution curves for $t = 0.25$. Right lower panel: The sub-solution and solution curves for $t = 0.4$.

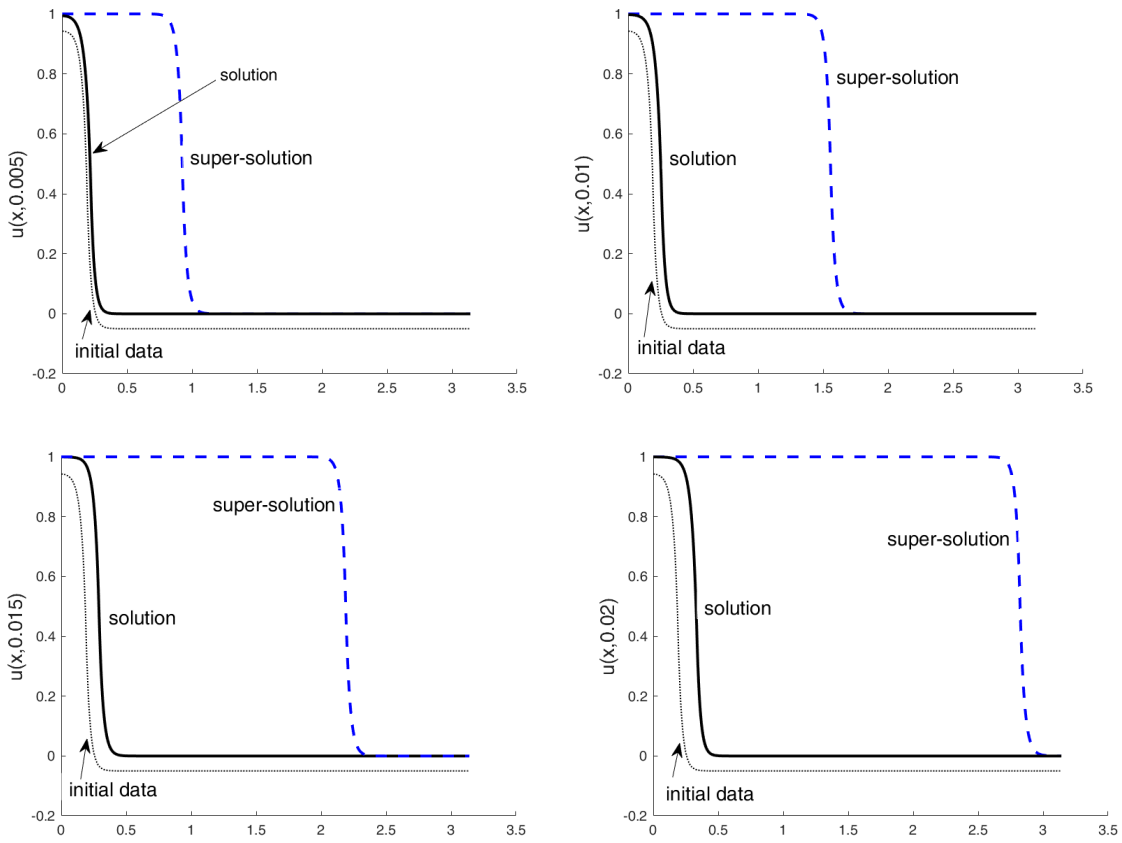

Figure 10: The dotted black curve corresonds to $U(x;\hat{\eta}_0,v)$, i.e. the initial sub-solution curve, and simultaneously the initial condition for Eq.(6). The dashed blue curves correspond to the super-solutions at given time and solid black curves depict the solution to Eq.(6). Left upper panel: The super-solution and solution curves for $t = 0.005$. Right upper panel: The subsolution and solution curves for $t = 0.01$. Left lower panel: The super-solution and solution curves for $t = 0.015$. Right lower panel: The super-solution and solution curves for $t = 0.02$.

2.5 Summary of the results

All three papers [B], [C], [E] consider analytical solutions to the traveling wave problem on the sphere.

In paper [B] exact analytical construction of stationary solutions to Eq. (3) was done, basing on the properties of the hypergeometric functions. In the paper we have proved that the constructed stationary solutions are unstable. This fact plays a key role in activation processes taking place on the cell membrane. The instability property was shown with the help of the theory of weak sub- and super-solutions. Using the explicit form of the stationary solution it was shown that for relatively small values of the diffusion coefficient (equivalent to large values of the parameter B), the profile of the stationary solution is changing abruptly with the small perturbations of parameter σ near $\sigma_0 = 0.5$ (see Figure 7). Because the stationary front is a separatix, we have to initially activate very small amount of receptors around the north pole of the of the sphere (corresponding to the angle $x = 0$) to induce the total activation of the cell in in the considered model (see Eqs. (1.3)-(1.4) in the paper [B]).

In the papers [C],[E] we have described, among others, the construction of the traveling wave like solutions to Eq. (3) generated by monotonic initial data. To examine their smoothness, we used the mild solution approach and analysed the infinite series of the Legendre polynomials together with the series obtained by its formal differentiation. The form of this series was complicated due to the discontinuity of the reaction term. Finally, the weak sub- and super-solutions were built. It was shown by numerical simmulations, that the time dependent solution lies between the constructed sub- and super-solutions, if only the initial data lie between them.

3 Wave front blocking in 3D and 2D domains - papers [D], [F]

3.1 Motivation

The motivation for the next papers are ubiquitous phenomena of pattern formation, in particular in diverse biological systems. Within the framework of reaction-diffusion description, spatial patterns may be understood as stable stationary solutions with non-zero gradients of concentrations, establishing polarization of the considered region or other forms of non-homogeneity in general. In majority of cases, pattern formation processes are opposite to diffusion phenomena, which tend to equalize the concentration to the average level. It was shown already in Casten and Holland[14], and in Matano[15] that stable non-homogeneous solutions of a single reaction diffusion equations with zero Neumann boundary condition in convex domains do not exist.

THEOREM *(Casten & Holland 1978) Suppose that* Ω *is a convex subset of* $\mathbb{R}^n$ *and* $u : \Omega \to \mathbb{R}^1$ *is a nonconstant equilibrium (stationary) solution of class* $C^3(\Omega)$ *of the problem*

$$\begin{aligned} \frac{\partial u}{\partial t} &= \Delta u + f(u) \qquad in \qquad (0,\infty)\times\Omega, \\ \frac{\partial u}{\partial n} &= 0 \qquad\qquad\quad on \qquad (0,\infty)\times\partial\Omega \end{aligned} \tag{49}$$

then u is unstable.

In the paper ([D]), we have successfully tested the hypothesis about the possibility of stopping traveling fronts in widening, concave parts of 3D channels, as in Figure 11. We also aimed to show that we can generate stable spatialy non uniform stationary solutions arising as a result of blocking traveling fronts in diverse 3D geometry domains (see Figure 14). It needs to be stressed, that such blocking is just the result of local widening of channels, i.e. the effect of influence of purely geometrical properties on the front propagation. The consequences of such a phenomenon may be far-reaching. It is described by a relatively simple model including only one reaction-diffusion equation. However, it can incorporate also an influence of geometry and its time changes on the evolution of biological systems. The model does not go deeper into molecular level but may be a good heuristic hint for developing novel models of pattern formation. The similar hypothesis about the possibility of stopping traveling fronts on 2D boundaries of channels (at its concave parts) has been checked in the paper ([F]). Another result of this paper concerned modeling the influence of polarization of the surface on polarization of the volume by suitable system of reaction diffusion equations. Finally we aimed to characterize the curves of stationary front localization.

3.2 Main results

3.2.1 Wave front blocking in 3D domains - paper [D]

Polarization of concave domains by traveling wave pinning
Białecki S, Kaźmierczak B., Lipniacki T
PLOS ONE **12**, 12, e0190372-1-10 (2017)

Pattern formation is one of the most common and the most important fundamental phenomena in biology at various spatial and temporal scales. The spatial structures appear in a natural way in the population dynamics of living organisms, play a key role in the processes of morphogenesis, and are also closely related to the processes of signal transmission inside cells. Gradients of spatial concentrations of the relevant proteins may regulate the processes of cell division and cell movement. We propose a simple polarization mechanism described by a single reaction-diffusion equation. The main difference between the proposed mechanism and Turing bifurcation is revealed in the fact that it allows for the establishment of concentration gradients in specific sub-regions of the region under consideration.

Consider a scalar reaction-diffusion equation with homogeneous Neumann-type boundary conditions:

[14] Casten, R. G. & Holland, C. J. Instability results for reaction diffusion equations with Neumann boundary conditions. *Journal of Differential Equations* **27,** 266–273. doi:10.1016/0022-0396(78)90033-5 (1978).

[15] Matano, H. Asymptotic behavior and stability of solutions of semilinear diffusion equations. *Publications of the Research Institute for Mathematical Sciences* **15,** 401–454. doi:10.2977/prims/1195188180 (1979).

$$\begin{aligned} \frac{\partial u}{\partial t} &= D\Delta u + f(u) \qquad \text{in} \quad [0,\infty)\times\Omega \\ \frac{\partial u}{\partial n} &= 0 \qquad\qquad\quad \text{on} \quad [0,\infty)\times\partial\Omega. \end{aligned} \tag{50}$$

To establish the attention, we choose f in the form

$$f(u) = (1-u)(1+u)(u+\epsilon), \quad \epsilon \in [0,1). \tag{51}$$

Lets assume that the heteroclinic traveling wave front being solution to the problem (50) is running in the domain Ω shown in Figure 11. As a result of interaction of the traveling wave front with the

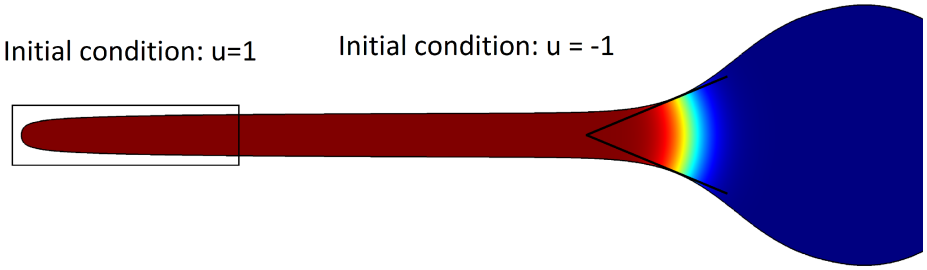

Figure 11: Initial conditions for traveling wave in 3D domain

inhomogeneous boundary[16] of the region (especially its concave pieces), this wave front may stop, establishing the polarization of the region. If we assume $D \ll 1$, this effect can be explained basing on the approximate formula for the effective front propagation speed[17].

$$\vec{v} \cong \vec{c} + D(\vec{\kappa}_1 + \vec{\kappa}_2), \tag{52}$$

where $\vec{c}$ corresponds to the 'one-dimensional' velocity, while $\vec{\kappa}_1, \vec{\kappa}_2$ are the local principal curvatures of the front surface. For regions Ω having the form of axially symmetric cylinders with variable intersection, the front surface is spherical, so $\kappa_1 = \kappa_2 = 1/R$, where R is the radius of the sphere.

Objectives and general strategy of numerical simulations

As we said, the main objective of the paper [D] was to show numerically that stable stationary spatially nonhomogeneous solutions to Eq.(50)-(51) can be obtained by traveling waves' pinning at concave parts of the channels, in which they are propagating. Moreover, as a sort of additional outcome of our numerical investigation, we wanted to check how precisely (52) is fulfilled depending on the magnitude of the coeffciecient D. It turns out that the effect of wave blocking is most easily generated for sufficiently small, *but nonzero* values of the diffusion coefficient D. For such values of D, the localization of the transition region (with width proportional to $\sqrt{D}$) and its radii of curvatures are relatively well determined. The transition region can be represented, for example, by the spherical surface $u(x,t) = -\epsilon$, to which the corresponding value of the curvature radius R can be assigned. In this way, we can find numerically the position of the wave pinning, and conclude that relation (52) is satisfied with relatively good accuracy. Though, blocking phenomena can exist also for bigger values of D, it follows straightforwardly from our calculations, that they may cease to arise for sufficiently large D, even if they should take place according to relation (52). Finally, it is also worthwhile to emphasize, that an alternative approach using the variational calculus is presented shortly in section Discussion of the paper [D].

Assuming that the front surface is spherical and locally perpendicular to the boundary of Ω we conclude that the radius of the front curvature equals

$$R(z) = r\sqrt{1 + \left(\frac{dr}{dz}\right)^{-2}} \tag{53}$$

as can be derived basing on Figure 12 .

Now, it follows from (52) and Figure 12 that given z_0

[16] Berestycki, H., Bouhours, J. & Chapuisat, G. Front blocking and propagation in cylinders with varying cross section. *Calculus of Variations and Partial Differential Equations* **55,** 44. doi:10.1007/s00526-016-0962-2 (2016).

[17] Tyson, J. J. & Keener, J. P. Singular perturbation theory of traveling waves in excitable media (a review). *Physica D: Nonlinear Phenomena* **32,** 327–361. doi:10.1016/0167-2789(88)90062-0 (1988).

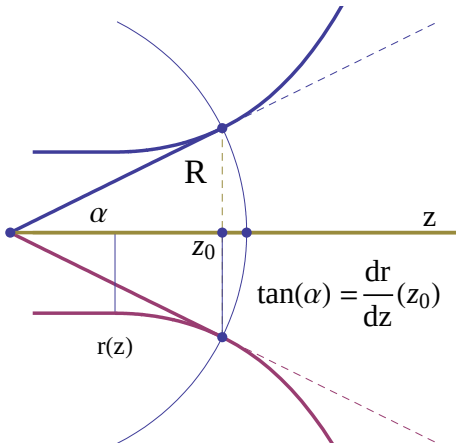

Figure 12: Derivation of Eq.(53) characterizing the radius $R(z_0)$ of the front sphere and its connection with the position z_0 where the front is stopping.

$$v(z_0) = c - \frac{2D}{R(z_0)}. \tag{54}$$

Using Eq.(54), we can conclude that a stationary front stopped at z_0, satisfies (for $D \ll 1$) the following relation between its radius and the velocity of the one dimensional plane wave

$$0 = c - \frac{2D}{R(z_0)}. \tag{55}$$

It is obvious that the stationary front is stable, if, for $|z - z_0|$ sufficiently small, $v(z) < 0$ for $z > z_0$ and $v(z) > 0$ for $z < z_0$. As $c = const$, then by means of relation (54), it implies that

$$\left(\frac{dR}{dz}\right)_{|z=z_0} < 0. \tag{56}$$

Condition (56) is equivalent to the inequality:

$$r'(z_0)^2 + r'(z_0)^4 < r(z_0)r''(z_0). \tag{57}$$

This inequality shows that the stable pinning takes place at sufficiently abrupt openings of the propagation channel.

Remark 3
Inequality (56) appears in the paper [D] as inequality (6) with opposite sign, but this difference was only due to the typographical error. □

Remark 4
The reaction diffusion Eq.(50) in spherical coordinates takes the form:

$$\frac{\partial u}{\partial t} = D\Big(\frac{\partial^2 u}{\partial r^2} + \frac{2}{r}\frac{\partial u}{\partial r} + \frac{1}{r^2\, sin\,\theta}\frac{\partial}{\partial \theta}\Big(sin\,\theta\frac{\partial u}{\partial \theta}\Big) + \frac{1}{r^2\, sin^2\,\theta}\frac{\partial^2 u}{\partial \phi^2}\Big) + f(u). \tag{58}$$

If u has spherical symmetry and does not depend on ϕ and θ, then in the vicinity of $r = R$ we obtain:

$$\frac{\partial u}{\partial t} \cong D\Big(\frac{\partial^2 u}{\partial r^2} + \frac{2}{R}\frac{\partial u}{\partial r}\Big) + f(u). \tag{59}$$

Assuming that the solution to Eq.(59) has locally the form of travelling wave $u(x,t) = u(r - vt)$ we obtain for $D \ll 1$:

$$D\frac{\partial^2 u}{\partial r^2} + \Big(D\frac{2}{R} + v\Big)\frac{\partial u}{\partial r} + f(u) \cong 0, \tag{60}$$

where from it follows that locally the solution is a travelling wave propagating with an effective speed

$$v = c - 2D\kappa, \tag{61}$$

where c is speed of the plane wave and $\kappa = 1/R$ is the curvature of the great circle on the sphere with the radius R in agreement with Eq.(52).

Moreover, using Lemma 2 from APPENDIX for $n = 3$, in the local coordinates (η_1, η_2) connected with a smooth two-dimensional hypersurface Σ and the perpendicular direction ξ at a given point $\mathbf{x}_0 \in \Sigma$, we can write Eq. (50) in the vicinity of this point in the form:

$$\frac{\partial u}{\partial t} = D\Big(\frac{\partial^2 u}{\partial \xi^2} + \frac{\partial^2 u}{\partial \eta_1^2} + \frac{\partial^2 u}{\partial \eta_2^2}\Big) + D(\kappa_1(\mathbf{x}_0) + \kappa_2(\mathbf{x}_0))\frac{\partial u}{\partial \xi} + f(u), \tag{62}$$

where by appropriate rotation of η_1 and η_2 axes, κ_1 and κ_2 can be considered as the main curvatures of the considered hypersurface Σ. Assuming that the solution to Eq.(50) has locally the form of travelling wave $u((\xi, \eta_1, \eta_2), t) = u(\xi - vt)$ we obtain for $D \ll 1$:

$$D\frac{\partial^2 u}{\partial \xi^2} + \Big(D(\kappa_1(\mathbf{x}_0) + \kappa_2(\mathbf{x}_0)) + v\Big)\frac{\partial u}{\partial \xi} + f(u) \cong 0, \tag{63}$$

from where, taking into account the directions of the vectors $\vec{\kappa}_1(\mathbf{x}_0)$ and $\vec{\kappa}_2(\mathbf{x}_0)$, we obtain for $D \ll 1$ the approximate equality (52). □

For the source function $f(u) = (1-u)(1+u)(u+\epsilon)$ the 1D (or plane) traveling wave solutions of problem (50), i.e. solutions of the form $u(x,t) = u(x - ct) = \omega(\xi)$ are given explicitly (see, e.g.[18], (13.88))

$$\omega(\xi) = \frac{1 - H\exp(\xi/w_0)}{1 + H\exp(\xi/w_0)}, \tag{64}$$

for an arbitrary constant $H \neq 0$, with front velocity c and front width $2w_0$

$$c = \epsilon\sqrt{2D} \quad \text{and} \quad w_0 = \sqrt{\frac{D}{2}}. \tag{65}$$

Then

$$\frac{1}{R(z_0)} = \frac{\epsilon}{\sqrt{2D}} \tag{66}$$

□

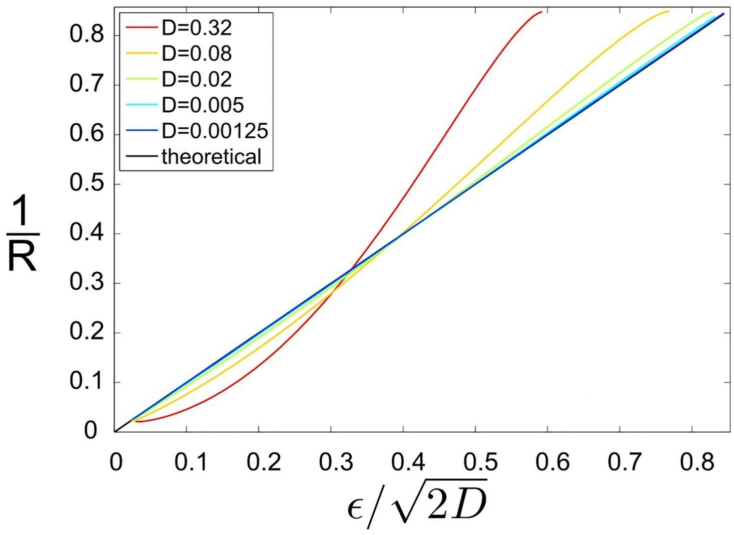

Figure 13: Characterization of the pinning position in the local widening of the domain Ω shown in Figure 11.

The accuracy of relation (66), has been checked numerically and illustrated in Figure 13, where the dependence of $1/R$ as a function of the ratio $\frac{\epsilon}{\sqrt{2D}}$ for the domain Ω in Figure 11 has been shown.

[18] Murray, J. D. *Mathematical Biology* (Springer-Verlag New York, 2002).

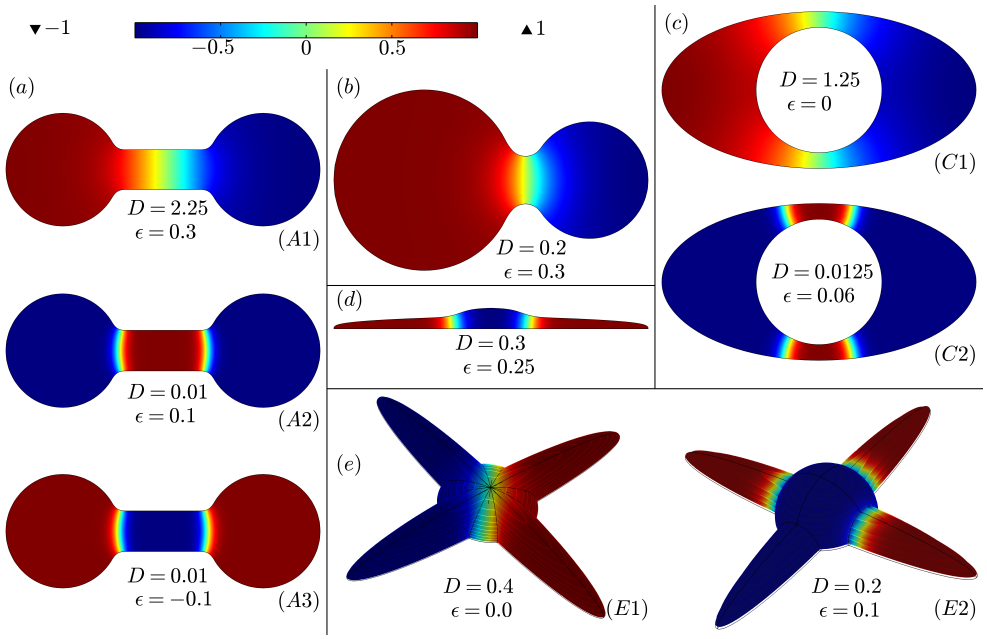

Figure 14: Nonconstant stationary solutions in different biological geometries obtained by traveling wave pinning: (a) **Bones**, (b) **Budding yeast cell**, (c) **cells with large nucleus (e.g. B-cells)**, (d),(e) **adherent cells**

Summary of the results

In the paper [D], we showed that heteroclinic traveling wave solutions to a scalar bistable equation of reaction-diffusion type with appropriately chosen parameters can stop on concave portions of the boundary of 3-dimensional domains. Depending on geometry, a number of stationary fronts may be formed leading to complex spatial patterns (as in the Figure 14). In contrast to the Turing bifurcation, the presented polarization mechanism is described by a single equation. Moreover, it allows for maintaining gradients of the analysed variables in the specific regions of the considered domain. If linking the instant domain shape with the instant spatial pattern, the mechanism can be responsible for cellular polarization and differentiation during morphogenetic processes. The work contains also a number of results of numerical simulations presented in Figure 14, which indicate the potential application of the proposed mechanism, e.g. to explain polarization processes of various types of biological structures at the cellular and tissue levels.

The numerical calculations have been carried out by means of the COMSOL Multiphysics (version 4.3 b) software. Additionally, I constructed appropriate Matlab scripts and the COMSOL LiveLink module for Matlab was used to obtain numerical graphs characterizing the blocking phenomena. □

3.2.2 Stopping of the wave front propagating on 2D domains - paper F

Traveling and standing fronts on curved surfaces
Białecki S, Nałęcz-Jawecki P, Kaźmierczak B, Lipniacki T
Physica D **401**, 132215 (2020)

In the paper, we analyze heteroclinic traveling waves propagating on two-dimensional manifolds formally described by reaction-diffusion equation with homogeneous Neumann-type boundary conditions:

$$\begin{aligned} \frac{\partial u}{\partial t} &= D\Delta u + f(u) \qquad \text{in} \quad [0,\infty)\times\Omega, \\ \frac{\partial u}{\partial \vec{n}} &= 0 \qquad\qquad\quad \text{on} \quad [0,\infty)\times\partial\Omega, \end{aligned} \tag{67}$$

where

$$f(u) = (1-u)(1+u)(u+\epsilon). \tag{68}$$

Here Ω is the 2D boundary surface of 3D domain (see Figure 15,16), $\epsilon \in [0,1)$, D is diffusion coefficient and Δ is the Laplace-Beltrami operator acting on Ω. The left hand side of the second equation denotes the directional derivative of u in direction $\vec{n}$ - normal to the curve $\partial\Omega$ limiting the surface Ω. The direction of $\vec{n}$ can be selected into the exterior of Ω and tangent to Ω. Starting with the step like initial condition, e.g. $u(\mathbf{x},0) = u_+$ to the left of the cross section perpendicular to the axis of the surface Ω and $u(\mathbf{x},0) = u_-$ to the right of this cross section (as shown in Figure 15) we can generate a solution achieving after some time the form of a traveling wave propagating on Ω joining the two steady states $u_- = -1$ and $u_+ = +1$.

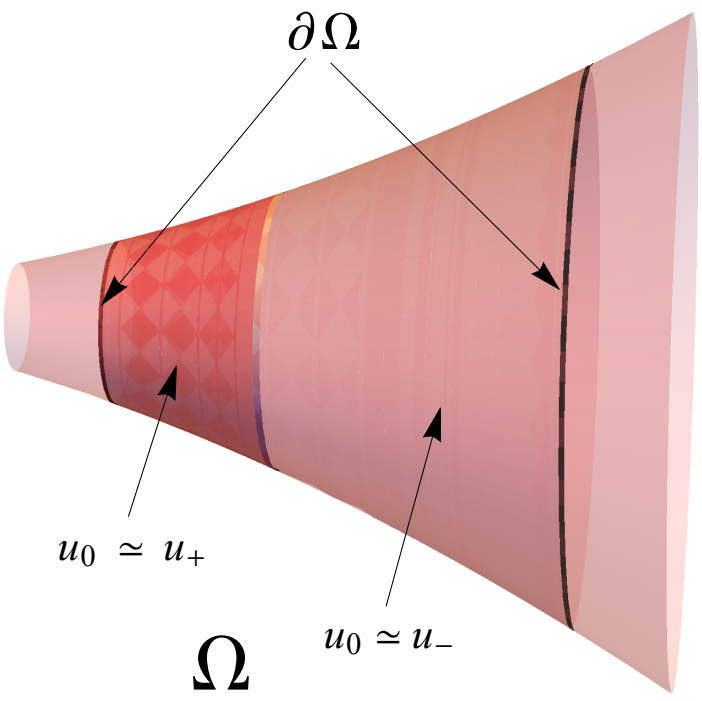

Figure 15: The schematic geometry considered in the paper F.

It is known[19][20],[21] that for fronts moving in the plane, the modification of their velocity with respect to the one dimensional speed is locally proportional to the curvature of the front line (see Eq.

[19] Zykov, V. S. Analytical evaluation of the dependence of the speed of an excitation wave in a two-dimensional excitable medium on the curvature of its front. *Biofizika* **25,** 888–892 (1980).

[20] Tyson, J. J. & Keener, J. P. Singular perturbation theory of traveling waves in excitable media (a review). *Physica D: Nonlinear Phenomena* **32,** 327–361. doi:10.1016/0167-2789(88)90062-0 (1988).

[21] Keener, J. P. A geometrical theory for spiral waves in excitable media. *SIAM Journal on Applied Mathematics* **46,** 1039–1056. doi:10.1137/0146062 (1986).

(1) in [F]). We propose a generalization of this rule for non plane surfaces. It consists in replacing the curvature of the front line with its geodesic curvature with respect to the surface by assuming that

$$\vec{v} \approx \vec{c} + D\vec{k}_g, \tag{69}$$

where $\vec{c}$ is the velocity of the one-dimensional traveling front solution for the first equation of (67) propagating in a plane locally tangent to the curved surface in a direction perpendicular to the front line. (For f given by (68), $|\vec{c}| = c$, where c is determined by the first equality in (65).) The geodesic curvature vector $\vec{k}_g$ is defined as the projection of the curvature vector $\vec{k}$ of the front line $\mathcal{L}$ on the plane locally tangent to the surface at the considered point. (Let us note that relation (69) appears also in Zykov[22].) If the wave is moving on the cone surface as in the Figure 15 in the direction of growing area of the cross section perpendicular to the symmetry axis then

$$v \approx c - Dk_g, \tag{70}$$

For the derivation of relation (70) in the case of axially symmetric surfaces, see Remark 5.

In view of Eq. (69), on the concave parts of the boundary hypersurface, stable stationary fronts can concentrate near curves of constant geodesic curvature. Eq. (69) becomes strict in the limit $D \to 0$. In this limit the stationary front lines ($v = 0$) tends to the corresponding lines of constant geodesic curvature $k_g = c/D = \frac{2\epsilon}{\sqrt{2D}}$. This fact has been numerically verified in the paper with a very high degree of accuracy (see Figure 18). The corresponding lines of constant geodesic curvature

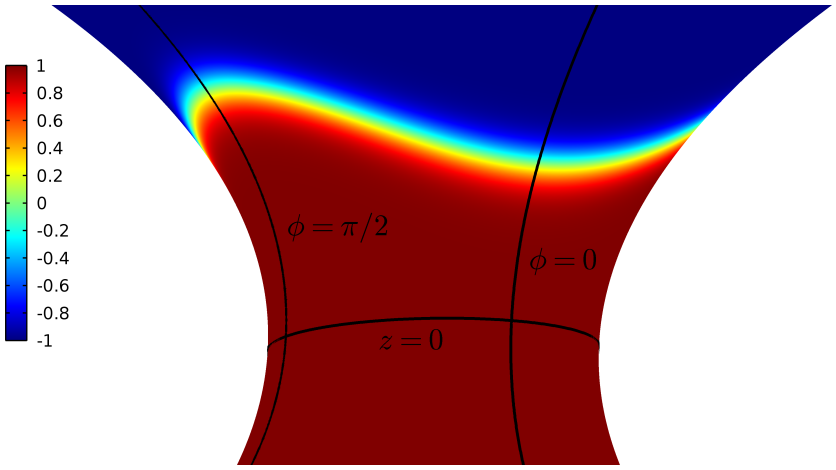

Figure 16: Characterization of stationary front on the surface $\mathcal{P}$ satisfying $x(z,\phi) = Qsin(\phi)(1+z^2)$; $y(z,\phi) = cos(\phi)(1+z^2)$

minimize the geometric functional describing the "energy" E (derived later in Eq.(75)) for the problem (67), consisting of two components: one proportional to the length L of the front line $\mathcal{L}$ and other to the area S_- of the surface $\mathcal{S}_-$, where the solution u is close to the lower stable point u_- and covered by the front line:

$$E = aS_- + bL.$$

It is convenient to parametrize the points on $\mathcal{L}$ by assigning to them the corresponding arc length l measured from a fixed point on $\mathcal{L}$. Let $\delta\xi(l) = \vec{m} \cdot \vec{\delta\xi}(l)$, where $\vec{m}$ is a unit vector in the direction tangent to the surface, normal to $\mathcal{L}(s)$, and directed from $\mathcal{S}_+$ to $\mathcal{S}_-$. The $\mathcal{S}_+$ is the surface (of the area S_+) where the solution u is close to the upper stable point u_+. The variational derivative of the functional E:

$$\delta E = a\delta S_- + b\delta L = \int_{\mathcal{L}} (-a + bk_g)\delta\xi dl + O(|\delta\xi|^2) \tag{71}$$

is zero if

$$k_g = a/b \tag{72}$$

and the front lines are stopping near lines of constant geodesic curvature. Hence a model establishes a mechanism for the formation of spatial patterns on surfaces. The values of parameters a and b can

[22] Zykov, V. S. Kinematics of rigidly rotating spiral waves. *Physica D: Nonlinear Phenomena* **238,** 931–940. doi:10.1016/j.physd.2008.06.009 (11–12 8th Sept. 2009).

be determined with the following reasoning. Let us see that:

$$D\nabla^2 u - \frac{\partial V}{\partial u} = 0, \tag{73}$$

is stationary counterpart of Eq.(67), where

$$V(u) = -\int_{(\cdot)}^{u} f(\mu)d\mu. \tag{74}$$

The potential V is specified in Eq.(74) up to an additive constant due to the arbitrary value of the lower integral limit in (74). From the physical point of view this constant is however not essential. For f given by (68) and $(\cdot)$ chosen as 0, we have

$$V(-1) = -\frac{1}{4} + \frac{2\epsilon}{3}, \quad V(+1) = -\frac{1}{4} - \frac{2\epsilon}{3}, \quad V(-1) - V(1) = \frac{4\epsilon}{2}.$$

The last quantity does not depend on the choice of the lower integration limit.

Eq.(73) may be obtained as the Euler-Lagrange equation from the following energy functional:

$$E[u] := \int_{\Omega} \Big(V(u(x)) + \frac{1}{2} D|\nabla\, u(x)|^2 \Big) dx. \tag{75}$$

Thus assuming the specific form of the front profile (64) and taking $H = 1$ we can obtain an approximation of $E[u]$ in the thin front limit:

$$E[u] = \frac{4}{3}\epsilon S_- + \frac{2\sqrt{2}}{3}\sqrt{D}L. \tag{76}$$

Hence

$$k_g = a/b = \frac{2\epsilon}{\sqrt{2D}}.$$

Moreover the following necessary condition for stability of stationary solution can be obtained in the form:

$$\frac{\partial^2 E}{\partial \xi^2}\Big|_{\xi=0} = \int_{\mathcal{L}(0)} \Big(-\kappa(l,0) - k_{g0}^2 \Big) dl > 0, \tag{77}$$

where l parametrizes the curve $\mathcal{L}$, ξ is the coordinate perpendicular to the curve $\mathcal{L}(0)$, $\kappa(l,0)$ is Gauss curvature of the surface in position $l, \xi = 0$ and k_{g0} is constant geodesic curvature for curve $\mathcal{L}(0)$. If $\mathcal{L}$ is to minimize E, the value of expression (77) must be positive, which is not possible if $\kappa > 0$ everywhere. Consequently, on surfaces with positive κ, such as boundaries of 3D convex domains, there are no stable stationary solutions not equal to constant. In particular, such solutions do not exist on the sphere. This fact is confirmed in our paper [B]. Thus, by Theorem 4.1 in [B] pp.1778-1779, the explicit stationary solution(12) of the problem (6),(7),(8) (corresponding to Eq.(2.1) in [B]), with F being bistable piecewise linear function, described in Lemma 1, is not stable.

It should be emphasized that (77) is only a necessary, but not a sufficient condition for the stability of the front line. That is because we have limited ourselves to perturbations ξ that are constant along the front lines.

Finally, when the perturbations $\delta\xi$ of the curve are not constant, but may depend on l, we can arrive at an appropriate expression for the second variation of the functional E in the form:

$$\delta^2 E = \int_{\mathcal{L}(0)} \Big((-\kappa(l,0) - k_{g0}^2)(\delta\xi(l))^2 + \frac{1}{2}\Big(\frac{\partial \delta\xi}{\partial l}\Big)^2 \Big) dl. \tag{78}$$

The above formula shows that the inequality

$$(-\kappa(l,0) - k_{g0}^2) > 0 \tag{79}$$

for every $l \in \mathcal{L}(0)$, where $\mathcal{L}(0) = \mathcal{L}(\xi = 0)$ is a sufficient (but not necessary) condition for the front stability. When deriving the sufficient condition and the necessary condition, we used the Gauss-Bonnet theorem.

In this way we have obtained the necessary condition (77) and sufficient condition (79) for front stability.

As in the 3D case considered in the paper [D], the presented pattern formation mechanism is also described by a single reaction-diffusion equation and combines the formation of the spatial polarization pattern with the internal geometry of the surface.

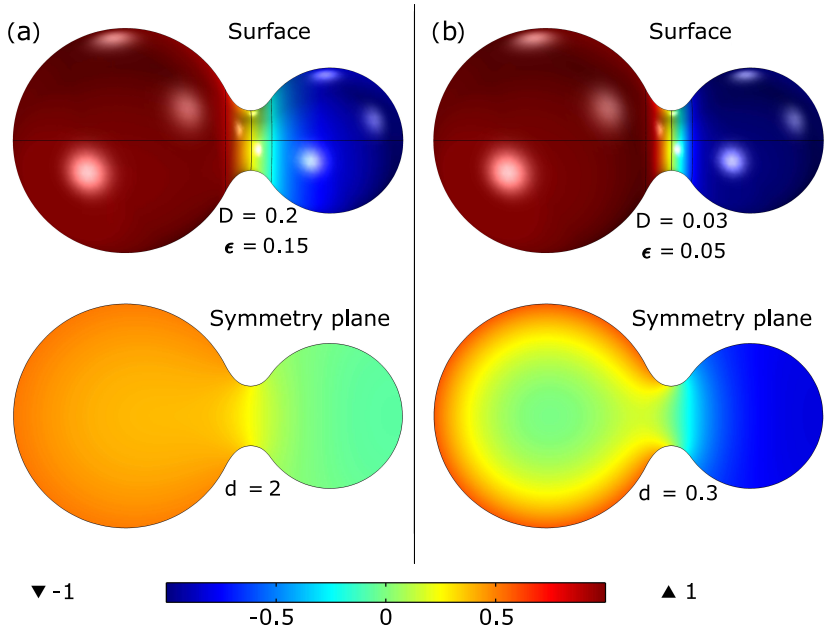

Figure 17: The polarization of the boundary surface $\partial\mathcal{C}$ generates the polarization of the entire volume $\mathcal{C}$. D - surface diffusion coefficient, d - spatial diffusion coefficient.

Moreover, we can show that the natural polarization of the surface can generate the polarization of the entire region, for which the surface is the boundary (see Figure 17). For this purpose, we consider a simple model in which the processes inside the cell $\mathcal{C}$ are coupled to the processes happening on the cell membrane $\partial\mathcal{C}$ by appropriate Robin-type boundary conditions.

So, we assume that on the cell membrane:

$$\frac{\partial u}{\partial t} = D\nabla^2 u + g(u) \qquad on \quad \partial\mathcal{C}, \tag{80}$$

with a bistable function g of the form

$$g(u) = 4u(u-1)\Big(\frac{1-\epsilon}{2} - u\Big). \tag{81}$$

We also assume that the kinase K concentration inside the cell is described by the equation

$$\frac{\partial K}{\partial t} = d\nabla^2 K - aK \qquad in \quad \mathcal{C}. \tag{82}$$

This equation is supplemented with a boundary condition depending on the membrane variable u:

$$\vec{n}\cdot\nabla K = bu(1-K). \tag{83}$$

These types of equations are often used in mathematical biology to describe signal transduction. In this context, the variable u represents the level of activation of membrane receptors, which is regulated through some nonlinear regulatory processes leading to the bistability of the function $g(u)$. The variable K represents the local concentration of activated intracellular kinases. Quantity $1-K$ is therefore the local concentration of non-activated kinases, activation of which through contact with activated receptors implies the flux of activated kinases $bu(1-K)$, where b is the activation rate. Factor a is the deactivation factor. D and d ($D < d$) are the diffusion coefficients of membrane receptors and intracellular kinases, respectively. As a rule, d is an order of magnitude larger than D. Numerical simulations showing the polarization of a volume $\mathcal{C}$ due to polarization just the volume boundary surface $\partial\mathcal{C}$ is shown in Figure 17.

Summary of the results

We have shown that, the polarization scheme designed in paper **D** works also in the case of 2-dimensional hyper-surfaces. Stationary fronts can emerge at parts with negative Gaussian curvature, on lines of constant geodesic curvature, for which an appropriately constructed energy functional E attains a local minimum. In the paper, we present a mathematical analysis of this functional,

in particular derive sufficient condition together with necessary condition for the stability of such stationary solutions.

From the biological point of view such stationary front lines separate regions of different polarization of the boundary surface, emerging, e.g. via local activation of membrane receptors. By considering a system of equations modeling boundary-volume interaction, we demonstrate that polarization of the boundary surface can induce a corresponding polarization inside the volume. □

Numerical methods

As in the case of paper [D] we used the COMSOL Multiphysics (version 4.3 b) software, together with the COMSOL LiveLink module for Matlab. Additionally, we used the Mathematica software to find the curve of constant geodesic curvature. It has been done by demonstrating numerically that the wave fronts being the results of COMSOL simulations indeed converge to a curve with a constant geodesic curvature in the limit of very low diffusion.

To check the validity of the calculations performed by the COMSOL built-in tools, we used the Laplace-Beltrami operator expressed in curvilinear coordinates on axially symmetric cylindrical surfaces. For completeness, in subsection 2. of APPENDIX we insert a short derivation of this representation.

Remark 5
Let us prove the validity of Eq.(69) in the case of an axisymmetric 2D surface and heteroclinic fronts. Note that, if l denotes the signed length of the curve obtained by the cross section with a chosen symmetry plane (see definition (92), point 2. of APPENDIX 6), we have

$$\frac{1}{r}\frac{\partial r}{\partial l} = \frac{1}{r}\frac{\partial r}{\partial z}\cdot\frac{\partial z}{\partial l} = \frac{1}{r(l)}\cdot\frac{\tan(\alpha(l))}{\sqrt{1+\tan(\alpha(l))^2}} = \frac{\sin(\alpha(l))}{r(l)} = k_g(l),$$

where $\alpha(l)$ is an angle between the line tangent to the curve $r(l)$ at the point $(r(l), l)$ and the symmetry axis (see also Figure 12), and $k_g(l)$ is the geodesic curvature of the circle $r(\phi) = const$ at this point on the surface. Let us assume that locally, close to the point $(r(l), l)$,

$$u(l,t) = u(l - vt). \tag{84}$$

In view of (93), the first equation of system (67) can be written as

$$\frac{\partial u}{\partial t} = D\frac{\partial^2 u}{\partial l^2} + Dk_g\frac{\partial u}{\partial l} + f(u). \tag{85}$$

Using (84), we obtain locally for $D \ll 1$

$$0 \approx D\frac{\partial^2 u}{\partial l^2} + (Dk_g + v)\frac{\partial u}{\partial l} + f(u)$$

hence finally

$$v = c - Dk_g \tag{86}$$

where c is the velocity of the plane wavefront in the direction of growing l. □

Remark 6
The form (93) of the Laplace operator has been used to double check the correctness of the numerical computations performed in the paper. These computations (Figure 17 and Figure 18) were carried out in the COMSOL MULTIPHYSICS by using the "Coefficient form boundary PDE" module and the "Parametric surface" module (for defining the geometry). To check the validity of the results, I designed a simple axisymmetric geometry as above and compared the computations obtained by "Coefficient form boundary PDE" module with the results obtained by the simpler COMSOL module "Coefficient form PDE" with the Laplace-Beltrami operator expressed in curvilinear coordinates. □

Curves of constant geodesic curvature.

Next, it seems worthwhile to explain, how the curves of constant geodesic curvature for the Figure 3 of the paper [F] (and Figure 18 below) were obtained. The curves presented in Figure 18 (b, c, d, e) constitute "visual evidence" of the statement that with the diffusion coefficient D decreasing to 0, the stationary front lines obtained as a result of solving the problem defined by Eqs.(67)-(68) converge to curves with constant geodesic curvature on the surface:

$$\mathcal{P} = \{(x,y,z) : x = Qsin(\phi)(1+z^2), y = cos(\phi)(1+z^2), (z,\phi) \in (-L,L)\times(0,2\pi]\}.$$

The stationary front lines of heteroclinic solutions to Eq.(67) were obtained by means of the COMSOL MULTIPHYSICS software. According to what has been said above, these curves may serve as 'COMSOL' approximation to the curves of constant geodesic curvature corresponding to the limit $D = 0$. Our strategy to show it, was to use the approximate values of $k_g^C \approx 2\epsilon/\sqrt{2D}$ assigned to the curve lines obtained with the help of the COMSOL software and perturbing them appropriately, to be able to obtain closed curves with constant geodesic curvature k_g. It turned out that using the MATHEMATICA software (and an original code) we were able to find k_g close to k_g^C such that the equation

$$k_g = \frac{(\boldsymbol{r}', \boldsymbol{r}'', \boldsymbol{n})}{|\boldsymbol{r}'|^3} \tag{87}$$

defining geodesic curvature[23],[24] for a curve given in the parametric form

$$\boldsymbol{r} : \phi \mapsto (r_1(\phi), r_2(\phi), r_3(\phi))$$

could be satisfied. In (87), (r_1, r_2, r_3) are Cartesian coordinates, $(\boldsymbol{r}^{'}, \boldsymbol{r}^{''}, \boldsymbol{n})$ is so called scalar triple product, and $\mathbf{n}$ is the local normal vector to the curve. The solution to Eq. (87) defines curves of constant geodesic curvature. The initial point of the curves (coinciding with the point of the original approximate curves) have been taken from the symmetry plane $\phi = 0$ of the surface $\mathcal{P}$, which allowed us to impose the condition $r_3'(0) = 0$ (where r_3 is equivalent to z). The obtained curves satisfied the conditions $\mathbf{r}(0) = \mathbf{r}(2\pi)$ and $r_3'(2\pi) = 0$, so they were smoothly closing after one turn around the surface $\mathcal{P}$. These results have been presented in panels (c), (d), (e) of Figure (18).

This analysis has been carried out for parameter ϵ (appearing in the definition of the function f (68)) taken from the set $\{\frac{\epsilon_{max} i}{50}, i = 1 \cdots 50\}$, where $\epsilon_{max} \approx 0.031$ is such that above that value no stationary front exists. For each such ϵ we obtained one stationary front using the COMSOL MULTIPHYSICS software and then with our MATHEMATICA code we proved that this front corresponds to the curve of constant geodesic curvature, which confirms the theory presented in the paper. In contrast to panels (c), (d), (e), in panel (b) we find the curve characterized by the geodesic curvature equal exactly to the theoretical value $2\epsilon/\sqrt{2D}$ by perturbing the localization of the starting point on the line of cross section $\mathcal{P} \cap \{\phi = 0\}$. The calculations were performed for $\epsilon = \epsilon_{max}/2$. It turns out that the coordinates z at points $\phi = 0$ and $\phi = \pi/2$ of the stationary wave front line (blue curve) are the most distant from the corresponding theoretical black curve of constant geodesic curvature. The discrepancy in these points is visualized in the panels (c) and (d) to illustrate the statement that asymptotically in the limit of small diffusion the curves of wave fronts converge to the curve of constant geodesic curvature. The panel (e) presents the difference between the real value of the curvature of the stationary front line for different values of ϵ and the theoretical value of the geodesic curvature (black line) in the limit of small diffusion in the axially symmetric ($Q = 1$) case.

[23]Struik, D. J. *Lectures on Classical Differential Geometry Second Edition* (Dover Publications, Inc. New York, 1988).

[24]Slobodyan, Y. S. *Geodesic curvature. Encyclopedia of Mathematics* Accessed on June 23, 2023. 2020.

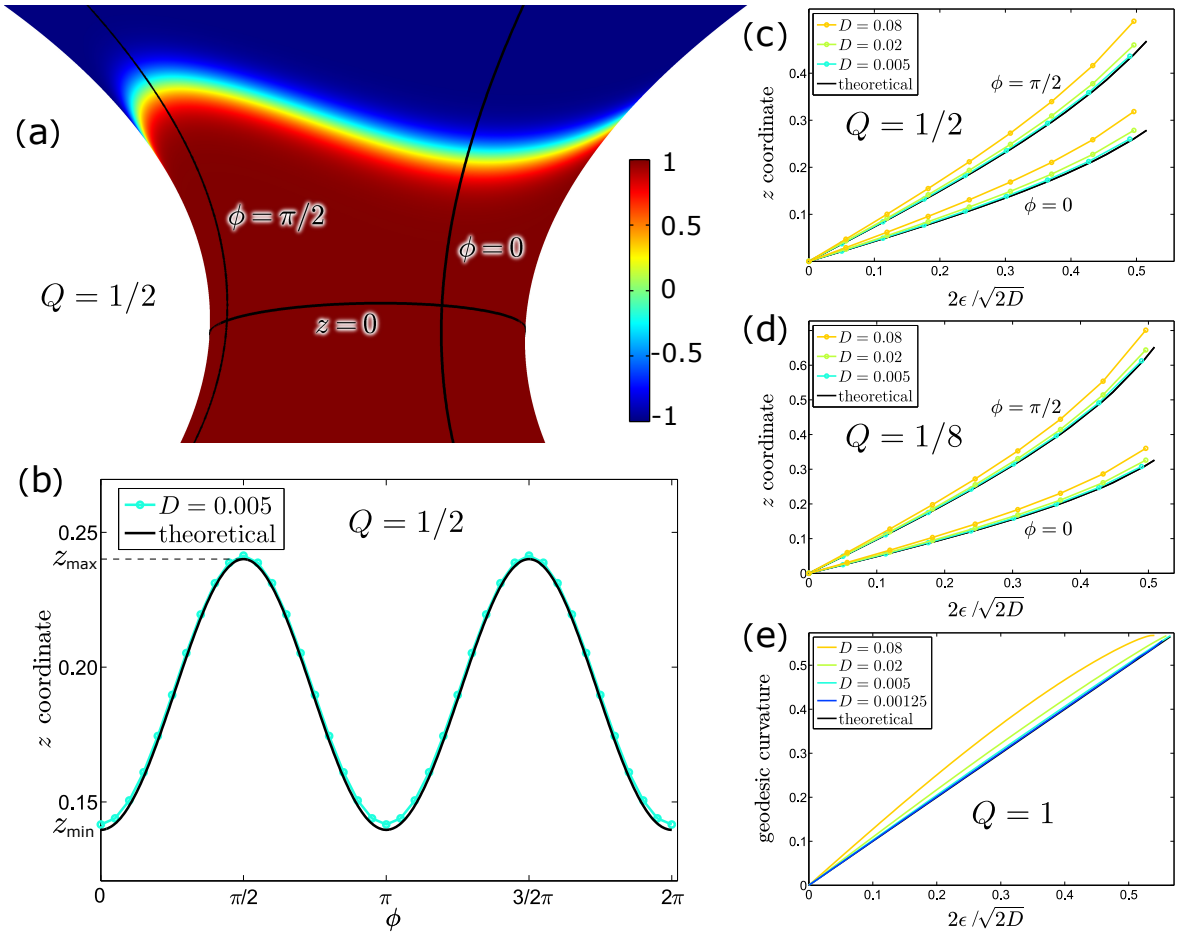

Figure 18: Characterization of stationary front on the surface $\mathcal{P}$ satisfying $x(z,\phi) = Q\sin(\phi)(1+z^2)$; $y(z,\phi) = \cos(\phi)(1+z^2)$. (a) Position of stationary front for $Q = 1/2, D = 0.005$, and $\epsilon = \epsilon_{\max} \approx 0.031$. (b) $z(\phi)$ for the stationary front line for $Q = 1/2, D = 0.005$, and $\epsilon = \epsilon_{\max}/2$. Numerical simulation (blue line) versus theoretical prediction in the limit of $D \to 0$ (black line). (c) and (d) z-coordinate of the stationary front for $\phi = 0$ and $\phi = \pi/2$ obtained in the numerical simulations (performed in COMSOL MULTIPHYSICS 4.3b) of Eq. (67) on $\mathcal{P}$ with the $Q = 1/2$ and $Q = 1/8$ versus theoretical predictions in the limit of $D \to 0$ (black line). (e) Geodesic curvature κ obtained in the numerical simulations on $\mathcal{P}$ with the circular cross-section (i.e. $Q = 1$) for four values of the diffusion coefficient D (color lines) versus theoretical prediction in the limit of $D \to 0$ (black line).

4 Podsumowanie

W pracach stanowiących podstawę niniejszej rozprawy przedstawiliśmy modele matematyczne (oraz ich analizę) wybranych zjawisk zachodzących w układach biologicznych. Immanentną cechą analizowanych procesów jest ich charakter przestrzenny. Podstawowym aparatem matematycznym użytym zarówno do sformułowania powyższych modeli, jak również do analizy postawionych problemów były równania reakcji-dyfuzji. Tematyka przedstawionych prac obejmowała zasadniczo dwa typy zjawisk: procesy związane z transdukcją sygnałów w strukturach biologicznych oraz procesy związane z formowaniem się wzorców przestrzennych. Oba typy procesów mają fundamentalne znaczenie w biologii. Pierwszy z nich jest podstawą funkcjonowania organizmów żywych w kontekście korelacji procesów biochemicznych w różnych obszarach komórki oraz między komórkami, umożliwia również adekwatne reakcje komórek na bodźce zewnętrzne. Drugi typ procesów jest nierozerwalnie związany ze zjawiskami kształtowania się organizmów żywych i ma kluczowe znaczenie w embriologii i morfogenezie. Zrozumienie mechanizmów różnicowania się komórek czy też formowania się wyspecjalizowanych narządów w tworzących się organizmach jest ciągle otwartym problemem zawierającym także ogromny ładunek filozoficzny. Pracami motywowanymi zagadnieniem przenoszenia sygnałów biologicznych są prace [B], [C] i [E], w których rozważamy procesy rozszerzania się obszaru zaaktywowanych receptorów na membranie komórkowej. W ramach zaprezentowanego modelu byliśmy w stanie ilościowo opisać efekty progowe oraz scharakteryzować propagację fali aktywacyjnej. Prace [A], [D] i [F] poświęcone są natomiast mechanizmom polaryzacji obszarów zachodzącym na skutek zmiennej, dostatecznie skomplikowanej geometrii obszarów. Oprócz analizy teoretycznej prace te zawierają szereg nietrywialnych przykładów przestrzennych i powierzchniowych struktur polaryzacyjnych w zaproponowanym mechanizmie zatrzymywania się fal biegnących. **Przedstawione prace pokazują, że modelowanie przestrzenne jest potężnym narzędziem, zapewniającym głębszy wgląd w bogactwo efektów związanych ze zjawiskami biologicznymi.** Moim zdaniem, są one dobrym punktem wyjścia do dalszych studiów w opisanych powyżej obszarach badawczych. W zakresie pierwszej grupy prac dobrze byłoby rozważyć propagację sygnałów na dowolnych zamknietych powierzchniach dwuwymiarowych z bardziej ogólną funkcją źródłową. W zakresie drugiej grupy prac naturalnym rozszerzeniem tematyki byłoby dołączenie efektów związanych z niejednorodnościami strukturalnymi ośrodków.

5 Conclusions

In the papers constituting the dissertation, we presented mathematical models (and their analysis) of selected phenomena occurring in biological systems. An immanent feature of the analyzed processes is their spatial character. The basic mathematical apparatus used both to formulate the models and to analyze the problems posed were reaction-diffusion equations. The topics of the presented works basically included two types of phenomena: processes related to signal transduction in biological structures and processes related to formation of spatial patterns. Both types of processes are of fundamental importance in biology. The first is the basis for the functioning of living organisms in the context of correlation of biochemical processes in different parts of the cell and between cells. It also enables cells to respond adequately to external stimuli. The second type of processes is intrinsically linked to the phenomena of the formation of living organisms and is crucial in embryology and morphogenesis. Understanding the mechanisms of cell differentiation or the formation of specialized organs in forming organisms is still an open problem, which comprises also a huge philosophical content. Works motivated by the problem of biological signals' transmission are papers **B**, **C** and **E**, in which we consider the processes of activation of receptors on the cell membrane. Within the framework of the presented model, we were able to quantitatively describe threshold effects and characterize the propagation of the activation wave on the sphere. The papers **A**, **D** and **F** are devoted to the mechanisms of polarization effects generated by varying and sufficiently complex spatial geometries. In addition to the theoretical analysis, these works contain a number of non-trivial examples of spatial and surface polarization structures in the proposed mechanism based on blocking of traveling waves. **The presented works show that spatial modeling is a powerful tool as it provides deeper insight into rich effects connected with biological phenomena**. In my opinion, these works are a good starting point for further studies in the research areas described above. In reference to the first group of papers, we plan to consider signal transduction phenomena on arbitrary closed 2 dimensional surfaces with a more general source function. In reference to the second group of papers, a natural generalization would take into account effects connected with structural heterogeneity of the media.

6 APPENDIX

1. Laplace operator in $\mathbb{R}^n$ in local coordinates connected with an $(n-1)$ dimensional hypersurface

Consider a hypersurface $S = \{(x_1, x_2, \ldots, x_n) : x_1 - \omega(x_2, \ldots, x_n) = 0\}$ defined in the vicinity of the point $\mathbf{x}_0 \in S$. Assume that the hyperplane $x_1 = 0$ is tangent to the hypersuface S at the point $\mathbf{x}_0$. It follows that

$$\frac{\partial \omega}{\partial x_i}(\mathbf{x}_0) = 0, \quad i = 2, \ldots, n. \tag{88}$$

Let

$$\xi = x_1 - \omega(x_2, \ldots, x_n) \quad \eta_i = x_{i+1} \quad \text{for } i = 1, \ldots, n-1. \tag{89}$$

Let us derive the expression for the Laplace operator Δ in the variables $(\xi, \eta_1, \ldots, \eta_{n-1})$ at the point $\mathbf{x} = \mathbf{x_0}$.

Lemma 2 *Suppose that (88) and (89) hold. Then at $x = x_0$:*

$$\Delta_{\xi,\eta_1,\ldots,\eta_{n-1}} = \Big(\frac{\partial^2}{\partial \xi^2} + \sum_{i=1,\ldots,n-1} \frac{\partial^2}{\partial \eta_i^2}\Big) + \sum_{k=1,\ldots,n-1} \kappa_k(\mathbf{x}_0) \frac{\partial}{\partial \xi}$$

where $\kappa_k(\mathbf{x}_0) := -\dfrac{\partial^2 \omega}{\partial x_{k+1}^2}(\mathbf{x}_0)$, $k = 1, \ldots, n-1$ are the principal curvatures of the surface S at $\mathbf{x} = \mathbf{x}_0$.

We have:

$$\frac{\partial}{\partial x_1} = \frac{\partial \xi}{\partial x_1}\frac{\partial}{\partial \xi} + \sum_{i=1}^{n-1} \frac{\partial \eta_i}{\partial x_1}\frac{\partial}{\partial \eta_i}.$$

and

$$\frac{\partial}{\partial x_k} = \frac{\partial \xi}{\partial x_k}\frac{\partial}{\partial \xi} + \sum_{i=1}^{n-1} \frac{\partial \eta_i}{\partial x_k}\frac{\partial}{\partial \eta_i}.$$

It follows that

$$\frac{\partial^2}{\partial x_1^2} = \frac{\partial \xi}{\partial x_1}\frac{\partial}{\partial \xi}\Big(\frac{\partial \xi}{\partial x_1}\frac{\partial}{\partial \xi} + \sum_{i=1}^{n-1} \frac{\partial \eta_i}{\partial x_1}\frac{\partial}{\partial \eta_i}\Big) + \sum_{i=1}^{n-1} \frac{\partial \eta_i}{\partial x_1}\frac{\partial}{\partial \eta_i}\Big(\frac{\partial \xi}{\partial x_1}\frac{\partial}{\partial \xi} + \sum_{j=1}^{n1} \frac{\partial \eta_j}{\partial x_1}\frac{\partial}{\partial \eta_j}\Big)$$

and

$$\frac{\partial^2}{\partial x_k^2} = \frac{\partial \xi}{\partial x_k}\frac{\partial}{\partial \xi}\Big(\frac{\partial \xi}{\partial x_k}\frac{\partial}{\partial \xi} + \sum_{i=1}^{n-1} \frac{\partial \eta_i}{\partial x_k}\frac{\partial}{\partial \eta_i}\Big) + \sum_{i=1}^{n-1} \frac{\partial \eta_i}{\partial x_k}\frac{\partial}{\partial \eta_i}\Big(\frac{\partial \xi}{\partial x_k}\frac{\partial}{\partial \xi} + \sum_{j=1}^{n-1} \frac{\partial \eta_j}{\partial x_k}\frac{\partial}{\partial \eta_j}\Big)$$

Due to (89) we have in some vicinity of $\mathbf{x}_0$:

$$\frac{\partial \xi}{\partial x_1} = 1, \quad \frac{\partial \eta_i}{\partial x_1} = 0, \quad \frac{\partial \eta_i}{\partial x_k} = \delta_{(i+1)k}, \quad \text{for } i \in \{1, \ldots, n-1\} \text{ and } k \in \{2, \ldots, n\},$$

and exactly at $\mathbf{x} = \mathbf{x}_0$, for $k = 2, \ldots, n$,

$$\frac{\partial \xi}{\partial x_k} = -\frac{\partial \omega}{\partial x_k} = 0.$$

We thus have at $\mathbf{x}_0$,

$$\frac{\partial^2}{\partial x_1^2} = \frac{\partial^2}{\partial \xi^2}$$

and, for $k = 2, \ldots, n$,

$$\frac{\partial^2}{\partial x_k^2} = \frac{\partial}{\partial \eta_{k-1}}\Big(\frac{\partial \xi}{\partial x_k}\frac{\partial}{\partial \xi}\Big) + \frac{\partial^2}{\partial^2 \eta_{k-1}} = -\frac{\partial}{\partial x_k}\Big(\frac{\partial \omega}{\partial x_k}\Big)\frac{\partial}{\partial \xi} + \frac{\partial^2}{\partial^2 \eta_{k-1}} = -\Big(\frac{\partial^2 \omega}{\partial x_k^2}\Big)\frac{\partial}{\partial \xi} + \frac{\partial^2}{\partial^2 \eta_{k-1}}.$$

Thus finally at $\mathbf{x} = \mathbf{x}_0$:

$$\Delta_{\xi,\eta_1,\ldots,\eta_{n-1}} \;=\; \Big(\frac{\partial^2}{\partial \xi^2} \;+ \sum_{i=1}^{n-1} \frac{\partial^2}{\partial \eta_i^2}\Big) \;+\; \sum_{k=1}^{n-1} \kappa_k(\mathbf{x}_0)\frac{\partial}{\partial \xi}$$

where

$$\kappa_k(\mathbf{x}_0) := -\frac{\partial^2 \omega}{\partial x_{k+1}^2}(\mathbf{x}_0) = -\frac{\partial^2 \omega}{\partial \eta_k^2}(\mathbf{x}_0), \quad k = 1, \ldots, n-1.$$

Let us note that

$$\sum_{k=1}^{n-1} \kappa_k(\mathbf{x}_0) = \sum_{k=1}^{n-1} -\frac{\partial^2 \omega}{\partial x_{k+1}^2}(\mathbf{x}_0) = \sum_{k=1}^{n-1} -\frac{\partial^2 \omega}{\partial \eta_k^2}(\mathbf{x}_0).$$

Now, the Laplace operator is invariant with respect to orthogonal transformations of the coordinates (in particular rotations) hence for $n = 3$ the last sum is equal to the sum of the principal curvatures of the surface S at $\mathbf{x} = \mathbf{x}_0$.

2. Laplace-Beltrami operator on axially symmetric surfaces

The Laplace-Beltrami operator in curvilinear coordinates has the following form:

$$\nabla^2 f = \sum_{i,j} \frac{1}{\sqrt{|g|}}\partial_i\Big(\sqrt{|g|}g^{ij}\partial_j f\Big), \tag{90}$$

where $|g| = \det(g)$ and g is a metric tensor, i.e. $ds^2 = g_{ij}dx^i dx^j$ and g^{ij} are the entries of the matrix g^{-1}. For the 2D axisymmetric hypersurface S, where S is given by the relation $r = r(z)$, we have $ds^2 = r^2 d\phi^2 + \Big(1 + \Big(\frac{dr}{dz}\Big)^2\Big)dz^2$, hence

$$g = \begin{pmatrix} 1 + \Big(\frac{dr}{dz}\Big)^2 & 0 \\ 0 & r^2 \end{pmatrix}.$$

In consequence, the Laplace-Beltrami operator acting on the function $f : S \to \mathbb{R}$ has the form

$$\nabla^2 f = \frac{1}{r\sqrt{1 + \Big(\frac{dr}{dz}\Big)^2}}\frac{\partial}{\partial z}\Big(\frac{r}{\sqrt{1 + \Big(\frac{dr}{dz}\Big)^2}}\frac{\partial}{\partial z}f\Big) + \frac{1}{r^2}\frac{\partial^2}{\partial \phi^2}f. \tag{91}$$

Now, let

$$l(z) = \int_{(\cdot)}^{z} \sqrt{1 + \Big(\frac{dr}{dz}\Big)^2}\,dz \tag{92}$$

denote the signed length of the curve obtained by the cross section of S with the symmetry plane. By means of (91), and the fact that

$$\frac{\partial z}{\partial l} = \frac{1}{\sqrt{1 + \Big(\frac{dr}{dz}\Big)^2}}$$

it follows that in the coordinates (l, ϕ) the Laplace-Beltrami operator on S reads:

$$\nabla^2 f = \frac{1}{r}\frac{\partial}{\partial l}\Big(r\frac{\partial f}{\partial l}\Big) + \frac{1}{r^2}\frac{\partial^2 f}{\partial \phi^2} = \frac{\partial^2 f}{\partial l^2} + \frac{1}{r}\frac{\partial r}{\partial l}\frac{\partial f}{\partial l} + \frac{1}{r^2}\frac{\partial^2 f}{\partial \phi^2}. \tag{93}$$

References

1. Marhl, M. *et al.* Complex calcium oscillations and the role of mitochondria and cytosolic proteins. *Biosystems* **57,** 75–86 (2000).
2. Volpert, A. I., Volpert, V. A. & Volpert, V. A. *Traveling Wave Solutions of Parabolic Systems* (American Mathematical Society, 1994).
3. Murray, J. D. *Mathematical Biology* (Springer-Verlag New York, 2002).
4. Gilding, B. & Kersner, R. *Travelling waves in nonlinear diffusion-convection-reaction* (Springer Basel AG, 2004).
5. Cantrell, R. & Cosner, C. *Spatial Ecology via Reaction–Diffusion Equations* (John Wiley & Sons, Ltd., 2003).
6. Pao, C. V. *Nonlinear Parabolic and Elliptic Equations* (Plenum Press, 1992).
7. Chatterjee, P., Glimm, T. & Kazmierczak, B. Mathematical modeling of chondrogenic pattern formation during limb development: Recent advances in continuous models. *Mathematical Biosciences* **322,** 108319. doi:10.1016/j.mbs.2020.108319 (Jan. 2020).
8. Mogilner, A. & Savinov, M. Crawling, waving, inch worming, dilating, and pivoting mechanics of migrating cells: Lessons from Ken Jacobson. *Biophysical Journal* **122.** doi:10.1016/j.bpj.2023.03.023 (Mar. 2023).
9. Igoshin, O. *et al.* Pattern formation and traveling waves in myxobacteria: Theory and modeling. *Proceedings of the National Academy of Sciences* **98.** doi:10.1073/pnas.221579598 (Jan. 2002).
10. Mogilner, A. & Odde, D. Modeling Cellular Processes in 3-D. *Trends in cell biology* **21,** 692–700. doi:10.1016/j.tcb.2011.09.007 (Dec. 2011).
11. Hecht, I. *et al.* Activated Membrane Patches Guide Chemotactic Cell Motility. *PLoS computational biology* **7,** e1002044. doi:10.1371/journal.pcbi.1002044 (June 2011).
12. Ben-Jacob, E. *et al.* Chemomodulation of cellular movement, collective formation of vortices by swarming bacteria, and colonial development. *Physica A: Statistical Mechanics and its Applications* **238,** 181–197. doi:https://doi.org/10.1016/S0378-4371(96)00457-8 (1997).
13. Brenner, M., Levitov, L. & Budrene, E. Physical Mechanisms for Chemotactic Pattern Formation by Bacteria. *Biophysical journal* **74,** 1677–93. doi:10.1016/S0006-3495(98)77880-4 (Apr. 1998).
14. Oelker, A. C. *Mathematical Modeling and Pattern Formation for Bacterial Colonies* PhD thesis (Technische Universität München, Fakultät für Mathematik, 25th Dec. 2017).
15. Keener, J. & Sneyd, J. *Mathematical Physiology I* doi:10.1007/978-0-387-75847-3 (Springer New York, 2009).
16. Carafoli, E. Calcium - A universal carrier of biological signals. *The FEBS journal* **272,** 1073–89. doi:10.1111/j.1742-4658.2005.04546.x (Apr. 2005).
17. Carafoli, E. & Krebs, J. Why Calcium? How Calcium Became the Best Communicator. *THE JOURNAL OF BIOLOGICAL CHEMISTRY* **291,** 20849–20857. doi:10.1074/jbc.R116.735894 (40 Sept. 2016).
18. Dyzma, M. *Modelowanie oscylacji stężeń jonów wapniowych w komórkach eukariotycznych z uwzględnieniem obszarów bezpośredniego kontaktu pomiędzy mitochondriami a retikulum endoplazmatycznym.* PhD thesis (IPPT PAN, 1st Nov. 2014).
19. Morciano, G. *et al.* Role of mitochondria-associated ER membranes in calcium regulation in cancer-specific settings. *Neoplasia* **20,** 510–523 (2018).
20. Yang, X. *et al.* Mitochondria-associated endoplasmic reticulum membrane: Overview and inextricable link with cancer. *Journal of cellular and molecular medicine* **27.** doi:10.1111/jcmm.17696 (Feb. 2023).
21. Bobrowski, A., Kazmierczak, B. & Kunze, M. An averaging principle for fast diffusions in domains separated by semi-permeable membranes. *Mathematical Models and Methods in Applied Sciences* **27** (Feb. 2016).

22. Ridgway, E. B., Gilkey, J. C. & Jaffe, L. F. Free calcium increases explosively in activating medaka eggs. *Proceedings of the National Academy of Sciences* **74,** 623–627. doi:10.1073/pnas.74.2.623 (Feb. 1977).

23. Hat, B., Kaźmierczak, B. & Lipniacki, T. B cell activation triggered by the formation of the small receptor cluster: a computational study. *PLoS Computational Biology* **7,** e1002197. doi:10.1371/journal.pcbi.1002197 (10 Oct. 2011).

24. Antonov, V. A., Kholshevnikov, K. V. & Shaidulin, V. S. Estimating the Derivative of the Legendre Polynomial. *Vestnik St. Petersburg University. Mathematics* **43,** 191–197. doi:10.3103/S1063454110040011 (4 Apr. 2010).

25. Casten, R. G. & Holland, C. J. Instability results for reaction diffusion equations with Neumann boundary conditions. *Journal of Differential Equations* **27,** 266–273. doi:10.1016/0022-0396(78)90033-5 (1978).

26. Matano, H. Asymptotic behavior and stability of solutions of semilinear diffusion equations. *Publications of the Research Institute for Mathematical Sciences* **15,** 401–454. doi:10.2977/prims/1195188180 (1979).

27. Berestycki, H., Bouhours, J. & Chapuisat, G. Front blocking and propagation in cylinders with varying cross section. *Calculus of Variations and Partial Differential Equations* **55,** 44. doi:10.1007/s00526-016-0962-2 (2016).

28. Tyson, J. J. & Keener, J. P. Singular perturbation theory of traveling waves in excitable media (a review). *Physica D: Nonlinear Phenomena* **32,** 327–361. doi:10.1016/0167-2789(88)90062-0 (1988).

29. Zykov, V. S. Analytical evaluation of the dependence of the speed of an excitation wave in a two-dimensional excitable medium on the curvature of its front. *Biofizika* **25,** 888–892 (1980).

30. Keener, J. P. A geometrical theory for spiral waves in excitable media. *SIAM Journal on Applied Mathematics* **46,** 1039–1056. doi:10.1137/0146062 (1986).

31. Zykov, V. S. Kinematics of rigidly rotating spiral waves. *Physica D: Nonlinear Phenomena* **238,** 931–940. doi:10.1016/j.physd.2008.06.009 (11–12 8th Sept. 2009).

32. Struik, D. J. *Lectures on Classical Differential Geometry Second Edition* (Dover Publications, Inc. New York, 1988).

33. Slobodyan, Y. S. *Geodesic curvature. Encyclopedia of Mathematics* Accessed on June 23, 2023. 2020.